The Faculty of Biomedical Engineering

Technion

Projects Conference

June 26, 2019

Abstracts

הטכניון - מכון טכנולוגי לישראל / הפקולטה להנדסה ביו-רפואית

TECHNION – Israel Institute Of Technology / The Faculty Of Biomedical Engineering

TECHNION
Israel Institute
of Technology

Dear all,

The Annual Projects Conference in Biomedical Engineering is hosted by the Faculty of Biomedical Engineering at the Technion – Israel Institute of Technology. As the Dean of the Faculty of Biomedical Engineering and as the project course staff, we are pleased and honored to welcome you here.

The conference is hosting 4th year students who are eager to present their year-long projects and to receive feedback from academic researchers, industrial experts, and their peers. These projects implement the medical, engineering, and scientific tools that the students have acquired and developed during their BSc journey in Biomedical Engineering.

The students aim to provide solutions that meet research and development needs in the Biomedical industries and research departments. Through working on their projects, students gained invaluable, hands-on experience. They had to work through technical challenges and adhere to strict standards comparable to those in a real-world setting.
We believe that this hands-on experience engages graduates with the Biomedical industry and/or the wide variety of Biomedical research in a very strong way encouraging multidisciplinary work that is vital to the students' futures.

Additionally, we encourage the students to think out of the box to initiate new solutions and help foster their entrepreneurship skills. Above all, these projects are a key element of the faculty vision which strives to strengthen the long-term cooperation between academia and industry leaders.

In this booklet we are introducing the abstracts of all presented projects. We wish all students rewarding careers and bright futures. We hope that one day they will take an active part in similar projects as professional mentors from both the industry and academia.

Kindest Regards,
Prof. Shulamit Levenberg, Faculty Dean
Prof. Netanel Korin, Course Instructor

List of Abstracts

(1) Nanoparticles for KRAS Driven Cancers- Optimization and Automation

Yuval Harris, Maytal Avrashami, Hagit Sason-Bauer, Arbel Artzy-Schnirman, Yosi Shamay
Faculty of Biomedical Engineering, Technion- IIT, Haifa, Israel

(2) Automated Process of Nanoparticle Preparation for Drug Delivery to Head and Neck Cancers

Auralie Abehssera, Natalie Cohen, Arbel Artzy-Schnirman, Hagit Sason-Bauer, Yosi Shamay
Faculty of Biomedical Engineering, Technion - IIT, Haifa, Israel

(3) The Effect of Flow on Exosome Secretion from Dental Pulp Stem Cells on 3D Scaffolds

Roee Samuel, David Shevach, Barak Zohar, Arbel Artzy-Schnirman, Shaowei Guo, Shulamit Levenberg
Faculty of Biomedical Engineering, Technion - IIT, Haifa, Israel

(4) Analysis of Biophysical Behavior of Protein Translocations Through Nanopores

Kenda Daghash, Karawan Halabi, Shilo Ohayon, Arbel Artzy-Schnirman, Amit Meller
Faculty of Biomedical Engineering, Technion - IIT, Haifa, Israel

(5) Seeding Cells in a Microfluidic Device of a Small Capillary Network

Ola Faris, Lama Hakim, Merav Belenkovich, Danielle Nemcovsky, Mark Epshtein, Daphna Marbach-Harpaz, Arbel Artzy-Schnirman, Netanel Korin
Faculty of Biomedical Engineering, Technion - IIT, Haifa, Israel

(6) Volatile Organic Compounds as Mediators of Cellular Communication

Ameer Lawen[1], Majd Machour[1], Dina Hashoul[2], Walaa Saliba[2], Arbel Artzy-Schnirman[1], Hossam Haick[2]
[1] Faculty of Biomedical Engineering, Technion - IIT, Haifa, Israel
[2] The Wolfson Department of Chemical Engineering, Technion - IIT, Haifa, Israel

(7) Prosthetic Control by an EEG-based Brain-Computer Interface

Adi Cohen[1], Dan Ben Yehuda[1], Oscar Lichtenstein[1], Shunit Polinsky[2], Igor Demchenko[2]
Firas Mawase[1], Yoav medan[3,4]
[1] Faculty of Biomedical Engineering, Technion - IIT, Haifa, Israel
[2] Faculty of Mechanical Engineering, Technion - IIT, Haifa, Israel
[3] Haifa3D Co-Founder and Chairman, Visiting Scientist, Technion - IIT, Haifa, Israel
[4] Faculty of Electrical Engineering, Technion - IIT, Haifa, Israel

(8) Design and Characterization of an Implantable 3D Microfluidic Device for Connecting Large Blood Vessels with Self-Assembled Capillaries

Netta Nahum, Barak Zohar, Oscar Lichtenstein, Shulamit Levenberg
Faculty of Biomedical Engineering, Technion – IIT, Haifa, Israel

(9) Inside Out – Accelerometers as a Noninvasive Method for Evaluating Respiratory Effort in Heart Failure Patients

Nitzan Shmueli, Alon Meissner, Anna Faingersh Klebanov, Amit Livneh,
Oscar Lichtenstein, Amir Landesberg
Faculty of Biomedical Engineering, Technion – IIT, Haifa, Israel

(10) Development of A System That Induces Controlled Stenosis in Artificial 3D Blood Vessel Model

Rana Abu Obeida, Wissam Kardosh, Hila Zukerman, Maria Khoury, Mark Epshtein, Oscar Lichtenstein, Netanel Korin
Faculty of Biomedical Engineering, Technion - IIT, Haifa, Israel

(11) An Automatically Fully Adjustable CAD Model of a Low-cost, 3D Printed Prosthetic Hand for Trans-Radial Amputations

Valeriia Kravchik[1], Yair Herbst[2,4], Oscar Lichtenstein [1], Yoav Medan[3,4]
[1] Faculty of Biomedical Engineering, Technion - IIT, Haifa, Israel
[2] Faculty of Mechanical Engineering, Technion – IIT, Haifa, Israel
[3] Faculty of Electrical Engineering, Technion – IIT, Haifa, Israel
[4] Haifa3D organization, Haifa, Israel.

(12) Detection of Genetic Disorder Mechanisms in the Sinoatrial Node via ECG and Advanced Signal Processing

Ofri Goldenberg[1], Yuval Ben Sason[1], Ido Weiser-Bitoun[1], Aviv Rosenberg[2], Yael Yaniv[1]
[1]Faculty of Biomedical Engineering, Technion – IIT, Haifa, Israel
[2]Faculty of Computer Science, Technion - IIT, Haifa, Israel

(13) An Accessible Recording System for Analyzing Cardiovascular Signals

Gal Shleifer[1], Yael Pistunovich[1], Aviv Rosenberg[2], Ido Weiser-Bitoun[1], Yaron Blinder[3], Yael Yaniv[1]
[1]Biomedical Engineering Faculty, Technion - IIT, Haifa, Israel
[2]Computer Science Faculty, Technion - IIT, Haifa, Israel
[3]Zebra Medical Vision Ltd, Kibbutz Shfayim, Israel

(14) Super Resolution Dynamic Microscopy: a 3D CNN Solution

Yan Ziselman[1], Mordechai Vaknin[1,3], Elias Nahme[1,2], Yoav Shechtman[1,2]
[1] Faculty of Biomedical Engineering, Technion - IIT, Haifa, Israel
[2] NanoBioOptics lab, Biomedical Engineering, Technion - IIT, Haifa, Israel
[3]Faculty of Medicine, IIT, Haifa, Israel

(15) Recognition in Ultra-Sound Images of the Region of Interest Around the Left Ventricle with Convolutional Neural Networks (CNN)

Ilan Misano[1], Michal Tamir[1], Alon Begin[1], Yaron Blinder[2], Dan Adam[1]
[1]Biomedical Engineering Faculty, Technion - IIT, Haifa, Israel
[2]Zebra Medical Vision Ltd. - Shefayim, Israel

(16) Semi-Automatic Classification of Short-Axis Views of the Left Ventricle in Ultrasound Recordings

Mor Finestine[1], Salomé Attali[1], Alon Begin[1], Ido Farhi[1], Yaron Blinder[2], Dan Adam[1]
[1] Biomedical Engineering Faculty, Technion - IIT, Haifa, Israel
[2] Zebra Medical Vision Ltd

(17) Respiration Signal Detection in Thermal Images Using Deep Learning and Image Processing

Noam Freundlich[1], Gadi Mendel[1], Tomer Czyzewski[2], Amit Livneh[1], Yonatan Savir[2]
[1] Faculty of Biomedical Engineering, Technion - IIT, Haifa, Israel
[2] Department of Physiology, Biophysics & Systems Biology, Technion- IIT, Haifa, Israel

(18) Advanced Methods in Functional Mapping of the Cerebral Cortex During Awake Craniotomy

Shaked Ron[1,2], Amit Livneh[1], [*]Firas Mawase[1], [*]Omer Zarchi[3]
[1] Faculty of Biomedical Engineering, Technion - IIT, Haifa, Israel
[2] Faculty of Medicine, IIT, Israel
[3] Intraoperative Neurophysiological Service, Rabin Medical Center, Israel
[*]equally contributed

(19) Examining Cardiopulmonary Interactions Prior to a Cardiac Arrest in Children

Yonatan Prat[1,3], Yuval Barzilai[1,3], Amit Livneh[1], Danny Eytan[2,3]
[1]Faculty of Biomedical Engineering, Technion - IIT, Haifa, Israel
[2]Pedriatic Intensive Care Unit, Rambam Health Care Campus
[3]Faculty of Medicine, Technion IIT

(20) Estimation of Thermal Acoustic Response of Brain Tissue to Focused Ultrasound Implementing Coded Excitation

Alisa Komleva, Yevgeniya Shteynman, Daniel Dahis, Amit Livneh, Haim Azhari
Faculty of Biomedical Engineering, Technion - IIT, Haifa, Israel

(21) Automatic Identification of the Optimal Reconstruction Phase for Coronary Arteries CT Images

Maya Israel[1], Noam Moshe[1], Amit Livneh[1], Eran Langzam[2]
[1]Faculty of Biomedical Engineering, Technion - IIT, Haifa, Israel
[2]Philips Healthcare Ltd., Israel

(1)

Nanoparticles for KRAS Driven Cancers- Optimization and Automation

Yuval Harris, Maytal Avrashami, Hagit Sason-Bauer, Arbel Artzy-Schnirman, Yosi Shamay

Faculty of Biomedical Engineering, Technion- IIT, Haifa, Israel

Introduction: Cancer is the second most common cause of death worldwide. One of the known causes for cancer is a mutation in the oncogene KRAS, which is responsible for cell signaling and controls cell proliferation through the MAPK pathway. As of now, there are only a few conventional treatments in use that inhibit KRAS pathway. Being extremely hydrophobic, these inhibitors impose a serious treatment hurdle, as drug administration method is exclusively limited to oral uptake. As such, systemic distribution throughout the body is inevitable, impacting KRAS is a vital pathway to all cells, therefore these oral-uptake drugs have dose limiting side effects. One method of reducing the side effects is using drug-loaded nanoparticles, which enable the drug to be administrated via the bloodstream. In addition, it can target cancer cells specifically as tumors have leaky blood vessels. Currently, most nanoparticles used in the clinic are made of 20% drug and 80% stabilizers and their development is based on manual formulation using trial and error optimization. Our innovation is a method to prepare nanoparticles that have inverse ratio - 80% drug with 20% super-stabilizers, in an automated process. We predict that using our particles, the treatment will be more effective and with less side effects.

Methods: We have developed a novel method to automatically prepare nanoparticles using a liquid handling robot (Andrew Alliance). We compared between the manual and automatic methods regarding the way the drug was added into the mixture. In the manual way, the drug was added drop-wised while mixing. With 'Andrew', the drug was quickly added with mixing by fast pipetting.

Nanoparticles were purified using either centrifugation or PD10 size exclusion chromatography. Particle size, stability and concentration of drug in the nanoparticles were measured using DLS and HPLC and compared between the two methods.

In order to evaluate the efficacy of the different nanoparticles, a cell viability assay was performed on KRAS mutated pancreatic cancer cells (KPC cell line). Nanoparticles uptake and cells viability were observed using LionHeart automated fluorescence microscope.

Results: Nanoparticles characterization shows that the new automated method combined with PD10 purification is superior in all parameters. Evaluation of the treated

cancer cells indicates that the nanoparticles penetrated the membrane but did not enter the nucleus. In addition, drug release by the nanoparticles was observed, which led to inhibited growth and decreased the viability of the cancer cells.

Conclusions: Automated preparation of nanoparticles proved to be superior than manual preparation. In addition, using PD10 to separate nanoparticles resulted in smaller and more stable nanoparticles than the conventional centrifugation.

Keywords: Nanoparticles, KRAS, Automated Formulation, Cancer Drug Delivery.

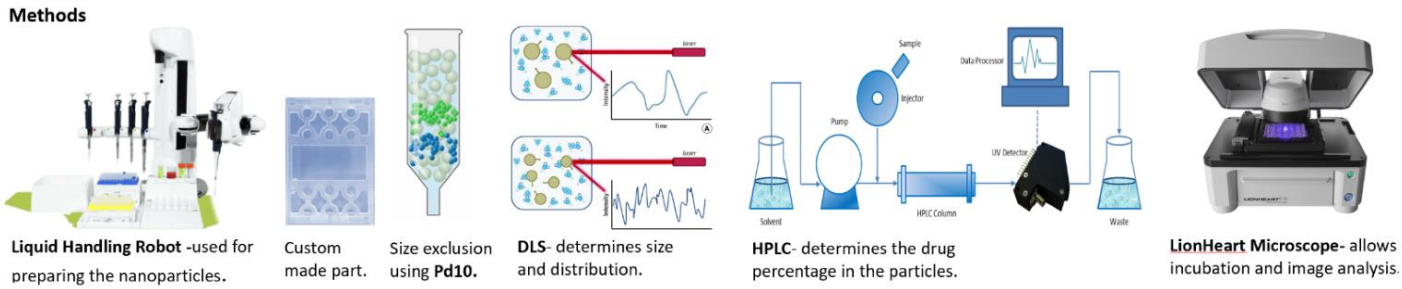

Figure 1: Methods used throughout the research.

(2)

Automated Process of Nanoparticle Preparation for Drug Delivery to Head and Neck Cancers

Auralie Abehssera, Natalie Cohen, Arbel Artzy-Schnirman, Hagit Sason-Bauer, Yosi Shamay

Faculty of Biomedical Engineering, Technion - IIT, Haifa, Israel

Introduction: Head and neck cancer is a group of cancers that affects the mouth, nose, throat, larynx, sinuses, or salivary glands. It is the sixth most frequent cancer with significant increase in incidents in recent years. Treatment for HNC usually includes chemotherapeutic drugs, which distribute to the entire body, resulting in toxic side effects that significantly degrade the quality of life in these patients.

Nanomedicine based on drug-loaded nanoparticles (NP) could potentially improve the treatment profile by delivery of high doses of the drugs to cancer cells while reducing side effects. Most nanoparticle formulation is based on manual trial and error, which is time consuming and tedious in order to find the optimal stabilizers and their ratio with a single drug.

In our research, we prepared NPs loaded with specific drug combination for Head and Neck cancer and developed a novel automated process of NPs preparation, using innovative tools.

Methods & Results: We first prepared NPs: we mixed a drug (Cabozantinib, Everolimus or the combination) with a stabilizer and then used a size exclusion chromatography method for NP purification. We discovered that this innovative method has advantages over centrifugation which is generally used for this purpose. We also observed that a new stabilizer, IR-595 is superior to all other stabilizers previously published (IR-820, IR-783). In addition, we showed that automatization by a liquid handling robot (Andrew Alliance) is possible in order to prepare large batches and combinations of NPs.

We characterized the properties of the NPs and evaluated their activity. We measured the stability of the NP over time, focusing on three parameters that DLS give us: Size, Mean Number and polydispersity index (PDI). The most stable NP formulation was Cabozantinib-IR595 with stability over one month in room temperature *(Figure 1a)*. We evaluated internalization and viability of the NP into cancer cells with an Automated Fluorescence Microscope (LionHeart) and observed that the NPs internalize into vesicles in the cytoplasm and present anti-tumor efficacy *(Figure 1b)*.

Conclusions: Automated process of NP preparation for drug delivery is feasible with Andrew, a novel liquid handling robot. It can automatically make a several batches of many NPs and represent a gain of time and precision in the process. One of the main steps of the preparation process is NP purification, classically using a centrifuge. However, in order to automatize, we had to think about a new purification method that could be feasible by Andrew. We indeed proved that purification using a chromatography filtration by size with a PD10 column is possible, and even has a slight advantage on the centrifuge in terms of stability and enhanced anti-tumor in vitro efficacy. We also saw in our research that the best stabilizer for Head and Neck Cancers drugs is IR-595, a new stabilizer whose properties have not been explored before.

Keywords: Nanoparticles, cancer drug delivery, automated synthesis

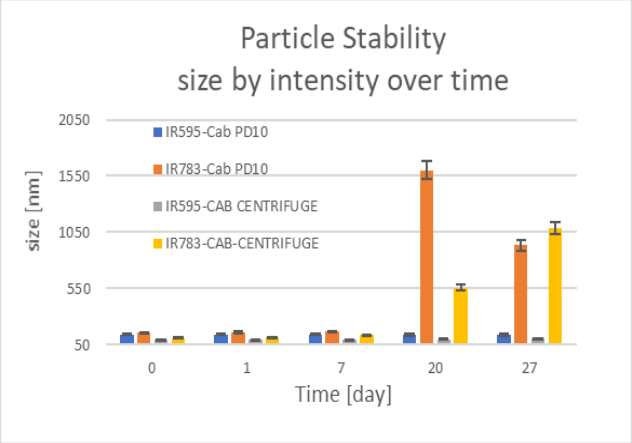

Figure 1a: Particle Stability size by intensity over time for Cabozantinib drug

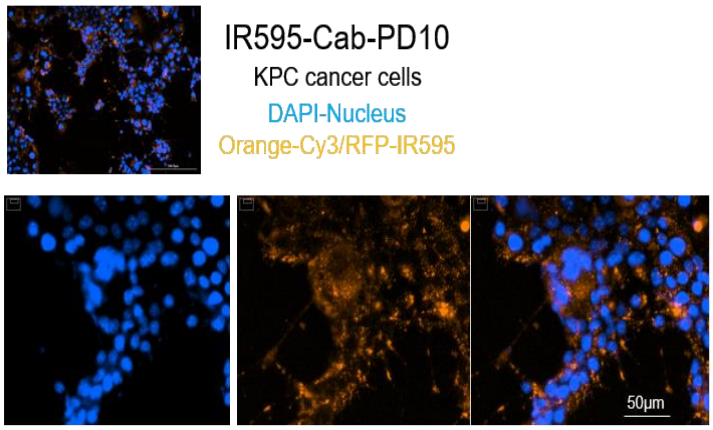

Figure 1b: internalization and viability of the NP into KPC cancer cells.

(3)

The Effect of Flow on Exosome Secretion from Dental Pulp Stem Cells on 3D Scaffolds

Roee Samuel, David Shevach, Barak Zohar, Arbel Artzy-Schnirman, Shaowei Guo, Shulamit Levenberg

Faculty of Biomedical Engineering, Technion - IIT, Haifa, Israel

Introduction: Exosomes recapitulate largely the therapeutic effects previously attributed to their parent cells. However, many important tasks remain before exosome therapy can be used clinically, including yield optimization. Perfusion bioreactor systems have been widely used to overcome limited mass transport in 3D cell cultures and for inducing physiological mechanical stimulation in the form of shear stress. In a recent study, a perfusion bioreactor system was utilized with 3D-printed scaffolds to enhance endothelial cell extracellular vesicle production. Dental pulp stem cells (DPSCs) are easily accessible stem cells from dental origin, with paracrine-mediated angiogenic and neuroregenerative properties.

In this study, we seeded DPSCs into off-the-shelf, GMP-compatible, 3D Fibra-Cel polypropylene /polyester scaffolds. The scaffolds were then assembled to a bioreactor with different flow rates. Under certain dynamic flows, exosome secretion from DPSCs on scaffolds was dramatically increased, compared to exosomes traditionally produced from 2D cultures or 3D static cultures.

Methods:

3D cell seeding and proliferation test: To optimize 3D cell seeding density, a series of DPSCs (0.05M, 0.1M, 0.2M or 0.4M, n=4/group) were seeded into Fibra-Cel scaffolds (15µm diameter fibers). Cell proliferation at days 3, 6, 9, 13 post-seeding was assessed using Alamar Blue assay. Cell number was calculated based on a calibration curve between Alamar Blue assay signal and known number of cells on scaffolds.

Bioreactor assembly and flow experiments: 3D cell-seeded scaffolds with optimized seeding density and incubation period were randomly assigned and assembled to a bioreactor system with exosome-depleted medium and different flow rates. Experimental groups include 1). 0.1 ml/min flow rate; 2). 0.5 ml/min; 3). 1.0 ml/min; 4). 3D static control (static flow); 5). 2D control (cells on 2D, without scaffolds). After two days, conditioned medium was collected for exosome isolation.

Exosome isolation and characterization: Exosome isolation was done with a differential centrifugation protocol (Figure1A). Exosome concentration and size distribution were measured using NanoSight instrument. Exosomes were analyzed by

Western blot, side-by-side with whole cell lysate, using anti-CD63 and anti-TSG101considered as exosome markers.

Results: When cell-embedded scaffolds were exposed in the 0.5 ml/min or 1.0 ml/min flow condition, there was up to 30 or 60 fold increase in the number of exosome per cell, respectively. Additionally, compared to the 2D control, cells grown on 3D scaffolds had a 1.5-fold increase in exosome number per cell.

Conclusions: Under certain flow conditions, a substantial number of exosomes could be generated from cell-embedded scaffolds, holding promises to overcome exosome yield limitations. Additionally, 3D scaffold enhanced DPSC exosome production compared to 2D environment.

Future experiment would investigate the mechanism and cargo of exosomes changed by shear stress, and whether these bioreactor-inspired exosomes could function better than exosomes traditionally harvested from 2D conditions, in preclinical models.

Keywords: Exosomes, DPSC, Bioreactor, Shear stress

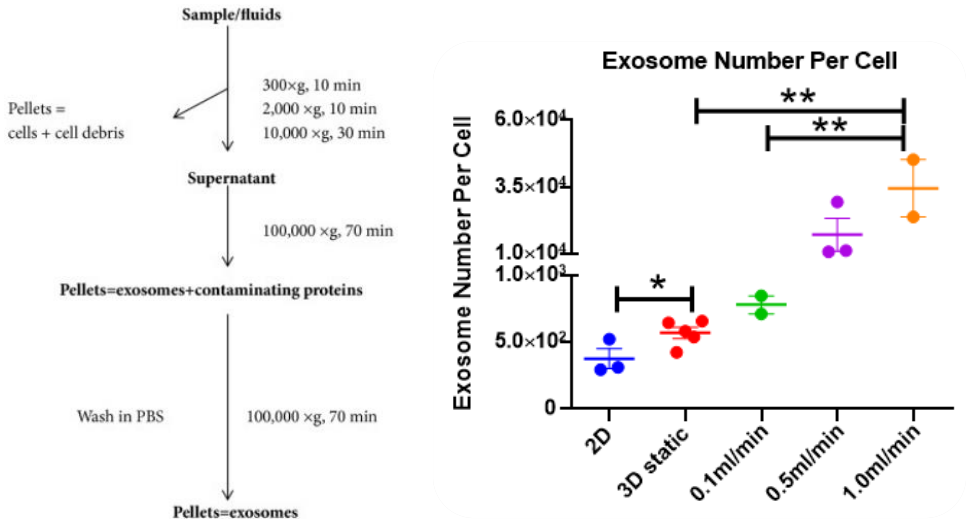

(A) (B)

Figure 1: (A) Exosome isolation protocol (B) Exosome number per cell from different groups.

(4)

Analysis of Biophysical Behavior of Protein Translocations Through Nanopores

Kenda Daghash, Karawan Halabi, Shilo Ohayon, Arbel Artzy-Schnirman, Amit Meller

Faculty of Biomedical Engineering, Technion - IIT, Haifa, Israel

Introduction: Single-molecule experimental techniques have recently shown to be of significant interest for use in both research laboratory and industrial settings. Although many single-molecule researches exist, the nanopore platform is perhaps one of the more popular techniques due to its ability to act as a molecular sensor of biological macro-molecules. Studies have primarily focused on understanding DNA transport kinetics and its implication on DNA sequencing. Nanopores have also found to be useful in the detection of small molecules, chemical reaction, synthetic polymers, and proteins. Currently, conventional methods for sequencing proteins, such as mass spectrometry and Edman degradation, suffer from short reads and lack sensitivity, so alternative approaches, such as nanopore analysis, are sought. The primary structure of a protein consists of a sequence of amino acids and is a key factor in determining how a protein folds and function. Here, we use Human serum albumin (HSA) – 585 A.A, 67kDa, as a control protein and one kind of cytokine protein TNFα – 157 A.A, 17.48 kDa, for detecting and characterizing the protein at the single-molecule level using nanopores.

Methods: In this method, an electric field induces electrophoretic translocation of protein molecules through nanopore that is slightly larger than the protein molecule. High-bandwidth ion current measurement is used to detect the transit of each protein molecule. Here, we show that a nanometre-diameter pore, sputtered through a thin silicon nitride membrane, can be used to detect the primary structure of denatured protein molecule. First, we check out whether the chips are intact using an optical microscope. Next, we need to remove any organic debris from the chips using Piranha; a mixture of sulfuric acid (H_2SO_4) and hydrogen peroxide (H_2O_2). After rinsing the chip with Deuterium-depleted water (DDW) the chips are dried using vacuum and nitrogen gas. The next step is hydroxylation of the chip's surfaces using Plasma. After that, we adhesive the chips on inserts made from Teflon using silicon-based organic polymer.

Results: Examining the translocations mean time (t_{mean}) and the fraction of the blocking current (I_B) by the open current at the start (I_0) for 3 different voltages for the two proteins; 150mV, 300mV and 450mV at roughly the same nanopores diameter ~3nm. Summarized noticeable results:

Voltage (mV)	t_{mean} (µsec) for TNF-α translocation	$\frac{I_B}{I_0}$ for TNF-α	$\frac{I_B}{I_0}$ for HSA
150	870	0.89	0.84
300	558	0.84	0.83
450	218.5	0.79	0.71

Conclusions: We compare the fraction $\frac{I_B}{I_0}$ and the t_{mean} for the two proteins at the same voltage;300mV. We observe that most of the proteins from the two kinds were fully denatured and had almost the same blockage. The t_{mean} of HSA protein had higher translocation time than TNF- α (as in figure1) and as the voltage increases, the t_{mean} decreases.

Keywords: Nanopores, protein translocations, electrophoreses.

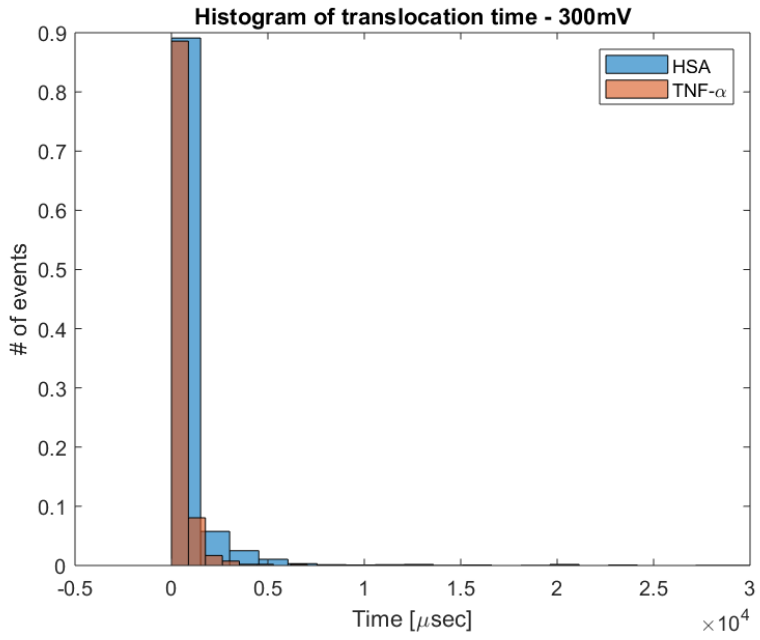

Figure 1: Histogram of translocation time at 300mV for HAS and TNF-α.

(5)

Seeding Cells in a Microfluidic Device of a Small Capillary Network

Ola Faris, Lama Hakim, Merav Belenkovich, Danielle Nemcovsky, Mark Epshtein, Daphna Marbach-Harpaz, Arbel Artzy-Schnirman, Netanel Korin

Faculty of Biomedical Engineering, Technion - IIT, Haifa, Israel

Introduction: Lab-on-a-chip, based on micro-fluidic technology, offers the ability to form in-vitro models of human physiological systems for research and industrial application. An example for such applications is a microfluidic device that mimics the capillary networks and enables us to study their crucial role in different diseases. When cells are introduced into these models, the main challenge is to maintain their viability in the small dimensions of the models. In our capillary network made from the inert polymer Polydimethylsiloxan (PDMS), direct seeding of the endothelial cells has been shown to be unsuccessful and, thus it was suggested to seed the endothelial cells in an open channel. However, sealing of the open seeded channel and maintaining the viability of the cells is necessary for a concrete and reliable capillary model. In the current research, we have designed and fabricated a device which enables reversible sealing of a microchannel following the seeding of Human Umbilical Vein Endothelial Cells (HUVEC) in the microchannel.

Methods: A sealing device based incorporating magnets and utilizing magnetic forces to seal the channel was designed using Solidworks and 3D printed using clear resin. N35 magnets were glued to the device. Microchannels were fabricated from PDMS using specific channels mold. A Sealing test was conducted by injecting dye into the channel's inlet and tracking it. A sealing reversibility test was conducted by re-opening the channel, re-sealing, and injecting the dye once more. HUVEC were seeded and stained with DAPI and Phalloidin.

Results: When a sealing test on the magnet based device was conducted, a leakage to the adjacent channel was observed, hence sealing was not sufficient. Then a thin PDMS layer was added in order to enhance the sealing, and a successful sealing test was achieved. Furthermore, reversibility was demonstrated by re-sealing the channel.

HUVEC cells were successfully seeded and stained. Cells viability and normal morphology were demonstrated.

Conclusions: Reversible sealing and successful HUVEC seeding were achieved when integrating the magnetic force device with a thin layer of PDMS. Suggestions for an improved reversible sealing would include modifying the device by: a) minimizing the open access area to the channel, hence enlarging the pressing area and improving the sealing and b) using stronger magnets.

Keywords: Microchannels, PDMS, magnetic force, sealing, HUVEC.

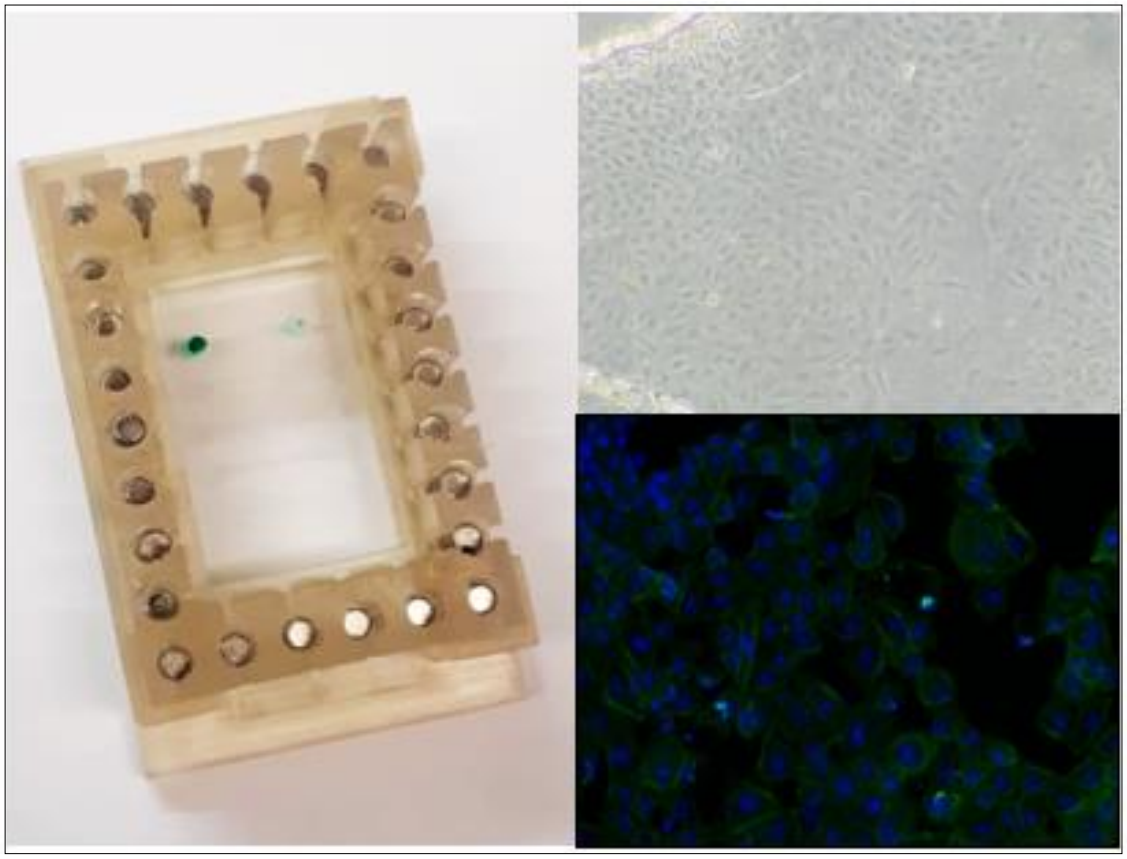

Figure 1: A reversible sealing device for microchannels based on magnetic forces with the assistance of a thin PDMS layer. Successful sealing (left) and enodthelail cells viability and normal morphology (right) were demonstrated.

(6)

Volatile Organic Compounds as Mediators of Cellular Communication

Ameer Lawen[1], Majd Machour[1], Dina Hashoul[2], Walaa Saliba[2], Arbel Artzy-Schnirman[1], Hossam Haick[2]

[1] Faculty of Biomedical Engineering, Technion - IIT, Haifa, Israel
[2] The Wolfson Department of Chemical Engineering, Technion - IIT, Haifa, Israel

Introduction: Volatile Organic Compounds (VOCs) are emerging as a new frontier in medical diagnostics for numerous diseases, and there have been documented success in their use as successful biomarkers for disease detection. This rests on the fact that VOCs express distinct and immediate changes in response to alteration in physiological processes. In addition, research has shown that VOCs play a role in the communication between plant cells and microbes. The question that arises from these established facts deals with whether specific VOCs are only a byproduct of cellular activity, or whether they have a role in the communication between cells in human tissues. Currently there is no commercial kit that enables us to examine this hypothesis, and therefore we aimed to optimize a method to validate the communication between well-studied A549 lung cancer cells, and U937 monocytes. the suggested method will enable us to explore VOC patterns emitted from a "sender cell" and how they affect a "receiver cell".

Methods: We used a Computer-aided designed (CAD) glass microfluidic chamber for the analysis of VOCs appearing in the headspace of cell cultures. The chamber consists of two wells separated by a check valve to ensure one-way transmission of VOCs between sender cells (A549) to receiver cells (U937). The headspace is sampled using a micropump and Tenax-filled glass adsorption tubes, which will be analyzed with Gas Chromatography – Mass Spectrometry. The optimization included the following: selecting Tenax material best suited for adsorption of cellular VOCs, the volume and concentration of cell suspensions, sampling time, and sampling flow rate.

Results: Tenax-TA with mesh size of 20/35 was found to be optimal in view of adsorption properties and flow obstruction, as seen by a higher number of peaks and higher area under curve in gas chromatographs. We identified 82 VOCs that significantly differed between test groups. 74 of these VOCs were found to be absorbed by monocytes (U937) when cultured with cancer cells (A549). Additionally, 8 VOCs were found to be emitted from monocytes when cultured with cancer cells.

Conclusions: The altered VOC profile of the monocytes after incubation with cancer cells with only a shared headspace suggests that there is indeed a potential for communication mediated by volatile organic compounds.

Keywords: Volatile Organic Compounds (VOC), Cellular Communication, Gas Chromatography – Mass Spectrometry (GCMS), 3D Printing

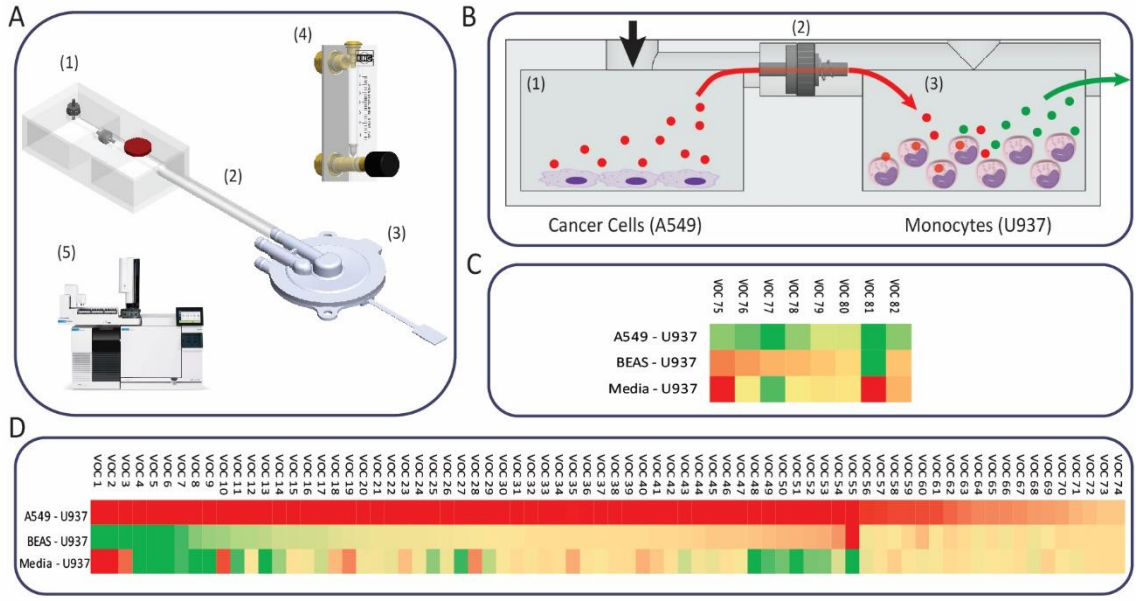

Figure 1: (A) Schematic overview of the system: 1. Glass chamber with one-way valve. 2. Gas adsorption tube. 3. Microfluidic pump. 4. Flow meter. 5. Gas chromatography – mass spectrometry. (B) Glass Chamber: cancer cells in sender well (1) emit VOCs (shown in red) through the one-way valve (2) to the monocytes in receiver well (3). These VOCs are consumed by the monocytes. In response to signals from cancer cells, monocytes emit VOCs (shown in green) that are sampled. (C, D) A heatmap showing the differences in VOC levels detected. Green represents more than 40% increase in VOC levels, red represents more than 40% decrease in VOC levels. The first, second and third lines show alteration in the VOC profile of monocytes when cultured with cancer cells, normal cells and media respectively.

(7)

Prosthetic Control by an EEG-based Brain-Computer Interface

Adi Cohen[1], Dan Ben Yehuda[1], Oscar Lichtenstein[1], Shunit Polinsky[2], Igor Demchenko[2]
Firas Mawase[1], Yoav medan[3,4]

[1] Faculty of Biomedical Engineering, Technion - IIT, Haifa, Israel
[2] Faculty of Mechanical Engineering, Technion - IIT, Haifa, Israel
[3] Haifa3D Co-Founder and Chairman, Visiting Scientist, Technion - IIT, Haifa, Israel
[4] Faculty of Electrical Engineering, Technion - IIT, Haifa, Israel

Introduction: Hand amputees cope with massive challenges in their life and suffer from lack of independence in performing daily operations, including some of the most mundane tasks. The main disadvantages of the prosthetic systems available today are need for residual nerve endings function, muscle activity or involvement of a different limb, phantom pain and high cost. Our project suggests an Electroencephalogram-based brain-computer interface (EEG-based BCI) as an enhanced control channel for prosthetic hands. The BCI application receives EEG input signal, analyzes them while extracting key features, and translates them into output control signals for the prosthetic device. This method requires only brain signals, and form an intuitive and possibly comfortable control channel.

Methods: For EEG signal acquisition, we used 64 EEG electrodes, eye tracker, 4 Electromyography (EMG) electrodes and flex sensor (potentiometer) to measure the physical movement of the hand throughout the trials. The data was recorded from healthy individuals instructed to open, close or rest their hands according to the color on the screen in sets of ten minutes, with a 2 seconds interval between adjacent gestures.

We pre-processed the acquired raw EEG signals to refine a clean viable signal, using notch filter (50Hz for power lines) and a band-pass, fourth order IIR Butterworth filter between 0.5-30 Hz, Conventional Recursive Least Squares (CRLS) to remove eye movement artifacts, interpolations of specific noisy channels. Using the flex sensor for timing, we divided the clean signal into 1-second-long Motion-Related-Potential segments, and labeled them accordingly.

Specific channels and frequencies were selected according to previous research, and according to the Event Related Potentials (ERP's), derived from the average response of numerous trials. Time domain features were mean, mean absolute deviation, variance and skewness. Frequency domain features included spectrogram at 0-20 HZ between -300 and 700 ms of movement onset.

We created different training datasets based on the experiments performed and randomly divided the data into 90 percent training, 10 percent testing. We employed classification models using the training data: k-nearest neighbors algorithm (k-NN), support-vector machines (SVM), NaiveBayes, Discriminant analysis and classification tree. We calculated the cross validation loss for each model and compared the prediction results, using measures as accuracy, sensitivity, specificity and precision.

In order to close the loop, we adapted the algorithm for real-time processing of EEG signals and connected it to the prosthetic hand using an Arduino interface.

Results:

Classification	Specificity	Sensitivity	Accuracy
Open vs. Close	72.22%	83.33%	79.17%
Movement vs. Rest	81.13%	83.72%	82.29%
Open vs. Close vs. Rest	71.43%	54.3%	63.64%

For classifying between open and close state and between movement and rest state **Discriminant Analysis classifier** showed best results, while for classification of 3 gestures **Classification Tree** was the best classifier.

Conclusions: Our project validates the feasibility of distinguishing between different hand positions, using discriminant analysis or classification tree. Further investigation needs to be done to allow real time control over prosthesis outside of lab environment.

Keywords: Brain-computer interface (BCI), Electroencephalography (EEG), Event related potential (ERP), Prosthetic hand, Motor cortex.

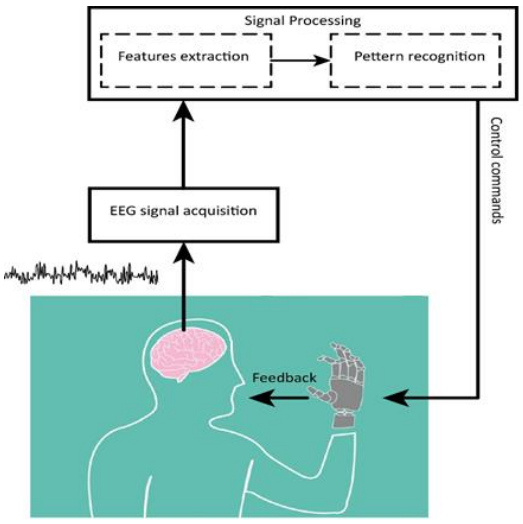

Figure 1: Process illustration of prosthesis control using EEG signal.

(8)

Design and Characterization of an Implantable 3D Microfluidic Device for Connecting Large Blood Vessels with Self-Assembled Capillaries

Netta Nahum, Barak Zohar, Oscar Lichtenstein, Shulamit Levenberg

Faculty of Biomedical Engineering, Technion – IIT, Haifa, Israel

Introduction: Vascularization of 3D engineered tissue has posed a great challenge in the field of tissue engineering: without proper blood supply, cells cannot survive in the depth of an engineered tissue due to the diffusion limitation. One approach for vascularizing engineered tissue is co-cultivation with Endothelial Cells (ECs). Under pro-angiogenic conditions, ECs spontaneously self-assembled into a capillary network. However, the self-assembled vasculature is not organized in the right hierarchy for supporting blood supply. An attempt for designing a perfusable organized vasculature has been successfully demonstrated by integrating micro-fluidic device with self-assembled capillaries. Yet, such devices are not suitable for implantations as they are neither biodegradable nor in a tissue scale.

A new approach for connecting large vessel with self-assembled capillaries is established at Shulamit Levenberg's lab. This approach is based on a biodegradable Polylactic acid (PLLA) 3D cylinder precisely perforated by a unique microfabrication technique ("AngioTube").

Our project goal was to design and characterize a system based on two AngioTubes, mimicking the artery and vein interface, to enable physiological blood flow through the self-assembled capillaries.

Methods: The system was designed using Solidworks. Flow velocity and shear stress were characterized by Computerized Fluid Dynamics (CFD) analysis using Ansys-Fluent. The system was fabricated by Polydimethylsiloxane (PDMS) using a 3D printed negative molding for assessing the flow using fluorescent beads tracking.

Results: Using CFD model, we simulated the maximal possible flow expected in the system. The system's parameters were chosen so that velocity values were included in the physiological range, and shear stress values were the minimal values of the physiological range [Table 1]. Too high shear stress in an under-matured vascular system might have negative effects on its growth.

By fluorescent particle tracking, the system's flow was characterized [Figure 1]. Values assessed were slightly smaller than the corresponding CFD values, as expected.

	AngioTube	CFD model	Fluorescent particle tracking	Physiological range
Velocity [mm/sec]	Artery-like	2±0.04	0.901±0.037	0-4
	Vein-like	1.9±0.06	0.792±0.098	
Shear stress [dyn/cm^2]	Artery-like	18.4±0.04	15±0.037	17-211
	Vein-like	17.5±0.09	13.2±0.098	

Table 1: Comparison of velocity and shear stress values for CFD model and fluorescent particle tracking compared to the physiological range by literature, for the two AngioTube's: artery-like and vein-like.

Conclusion: Using the CFD model we could successfully design a system that enabled us to reach physiological range velocity and shear stress. The design was tested by fluorescent particle tracking, and showed similar, slighlty lower values, as expected. This project has proved physiological flow can be achieved in the dual AngioTube system, to enable physiological blood flow through the self-assembled capillaries.

Keywords: Tissue vascularization, fluid characterization, micro fluidic device.

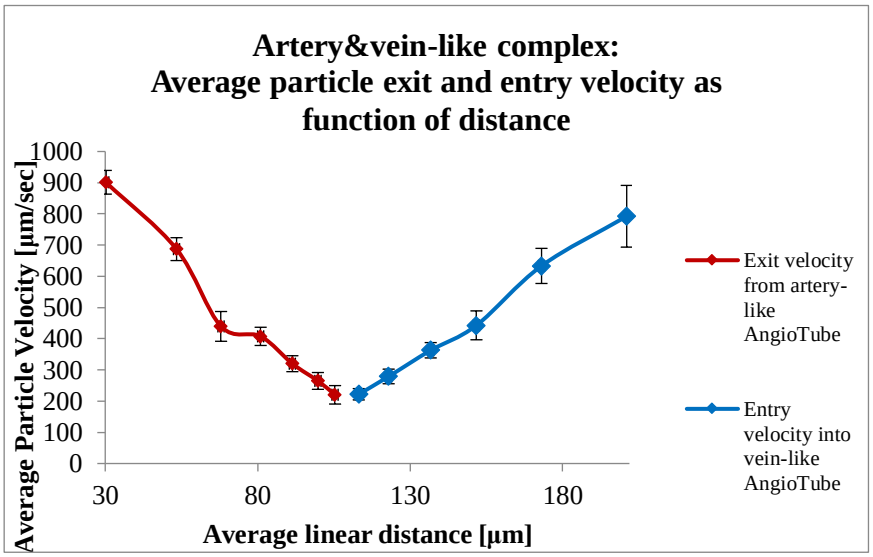

Figure 2: Flow velocity characterization by fluorescent bead tracking.

(9)

Inside Out – Accelerometers as a Noninvasive Method for Evaluating Respiratory Effort in Heart Failure Patients

Nitzan Shmueli, Alon Meissner, Anna Faingersh Klebanov, Amit Livneh,
Oscar Lichtenstein, Amir Landesberg

Faculty of Biomedical Engineering, Technion – IIT, Haifa, Israel

Introduction: Heart failure (HF) is a leading cause of mortality and morbidity. The most common complaint of HF patient is dyspnea, however, there are no tools to monitor it. The treatment is based on subjective symptoms and not on objective signs and consequently there are difficulties in optimization of treatment. Dyspnea relates to an increase in the respiratory effort (P_{RESP}). We hypothesized that the respiratory effort can provide measurable objective indices, that will revolutionize the management of HF. The objective is to quantify the severity of P_{RESP} by non-invasive body surface accelerometers and to extract indices that will tightly correlate with P_{RESP}.

Methods: Data were acquired during right cardiac catheterization, from 34 HF patients, at RAMBAM healthcare campus. The data included: air flow, pulmonary wedge pressure (PCWP), and motion dynamic from the accelerometers (f_S=1000[Hz]). The PCWP decomposed into respiratory and cardiac waves. The P_{resp} defined as the amplitude of the respiratory wave. We investigated the respiratory dynamics in the highest and lowest quartiles of the P_{resp} groups (n=12), in time and frequency domains. We implemented Welch's method to extract the power spectral density (PSD). The excessive effort index (EEI) was defined as the ratio of energy at high harmonics to the energy at the basic respiratory frequency band. The Flow was normalized to the body surface area.

Results: The respiratory dynamics of HF patients was complex and non-stationary. Excessive expiratory activity of the abdominal assessor muscles produced high energy above the basic frequency band. A tight correlation was found between EEI and P_{RESP}. EEI clearly classified and separated the low and high P_{RESP} groups. The P_{RESP} of the low and high P_{RESP} groups were: 5.27±1.46 and 13.55±0.67 mmHg, respectively. The EEIs of the low and high P_{RESP} groups were: 0.08±0.05 and 0.51±0.11 ($p<0.001$). interestingly, a significant inverse correlation was found between EEI and the Flow ($p<0.01$).
The HF patients develop respiratory effort ~5–fold larger than normal. The energy at the high frequency band of the respiratory dynamics vanishes at the P_{RESP}, suggesting that the efficiency of the transmission of muscle activity to P_{RESP} is low in HF patients. Patients with severe P_{resp} and large EEI produced lower airflow. Thus, the large P_{resp} is not transmitted efficiently into higher airflow. These observations may relate to the decrease in lung compliance and increase in resistance to flow. All the patients maintained normal saturation by increasing P_{RESP} and EEI.

Conclusion: Non-invasive monitoring of chest wall dynamics provides indices that quantify the severity of the respiratory effort. The ability to quantify the severity of HF by noninvasive means can significantly improve the surveillance of HF patients and may prevent rehospitalization.

Keyword: Heart failure; Dyspnea; Respiratory effort; Cardiopulmonary interactions.

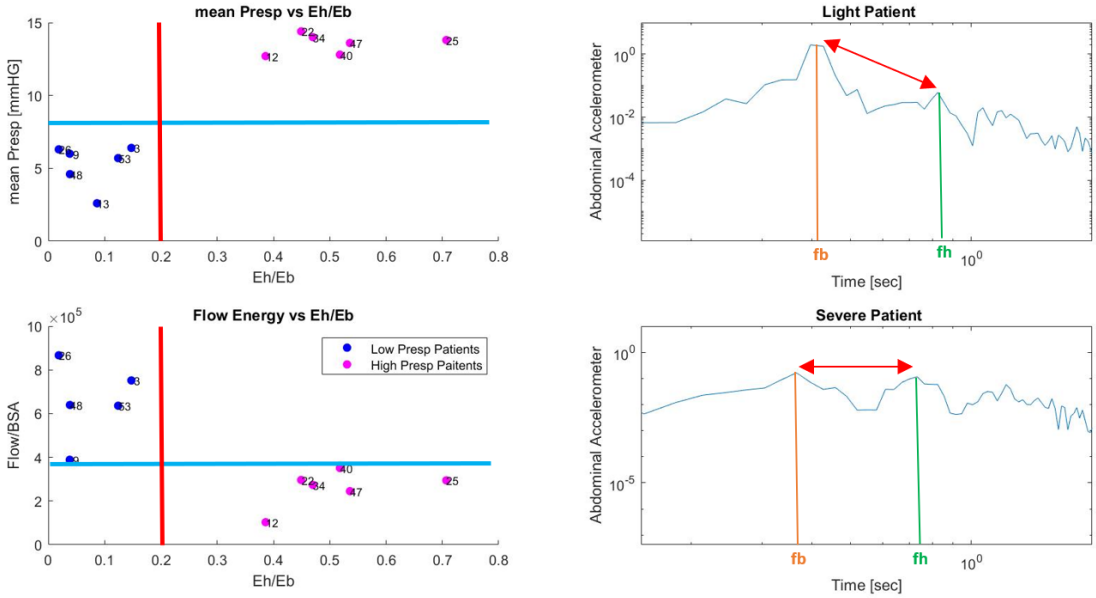

Figure 1: Main results: distinct separation by EEI (Eh/Eb), high P_{RESP} patients exhibited higher EEI and lower flow energy (p<0.01).

(10)

Development of A System That Induces Controlled Stenosis in Artificial 3D Blood Vessel Model

Rana Abu Obeida, Wissam Kardosh, Hila Zukerman, Maria Khoury, Mark Epshtein, Oscar Lichtenstein, Netanel Korin

Faculty of Biomedical Engineering, Technion - IIT, Haifa, Israel

Introduction: Cerebral Vasospasm is a potentially incapacitating or lethal complication in patients with aneurysmal subarachnoid hemorrhage (SAH). SAH causes stenosis of lateral vessels, which leads to ischemia and strokes. It affects about 10 out of 100,000 adults annually, and up to half of those affected die soon after. However, during the past decade the pathophysiology of delayed Vasospasm has progressed significantly, and intensive researches have been made in this area, this knowledge has not been translated into clinically effective treatment mainly because of the inadequate and ineffective animal or lab SAH models. Consequently, in our project we offer a new system that consists a 3D blood vessel model which stimulate stenosis by controlling external pressure on the vessel walls.

Methods: First, 3D blood vessel model were designed using Solidworks. Afterwards, the model was printed, which included the vessel and the pressure chamber, and was filled with transparent silicon polymer, PDMS, to obtain an artificial blood vessel (Fig. 1a). To apply pressure on the vessel's wall and induce stenosis:

1. Both the inner artificial blood vessel tube and pressure chamber were filled with solution containing 40% Glycerol: 60% DDW. This solution has approximately the same viscosity as blood.

2. In each step, an extra volume [indicated as System's Input] was added to the pressure chamber using a syringe. Thus, due to elasticity, an expansion occurred and triggered inducing of stenosis on the vessel wall.

3. Correspondingly, a certain volume was extruded from one side of the inner blood vessel tube [indicated as System's Output] and was measured using a pipette.

Results: We plot a calibration curve to determine what is the compressed required added volume to have a specific output. After that, we may convert the extruded volume to the pressure applied using fluid mechanics equations.

Conclusions: We were able to fabricate a 3D blood vessel while inducing controlled stenosis using applied pressure. By using this affordable device, we have successfully modeled a SAH condition, in which blood surrounds the brain vessels caused from ruptured cerebral aneurysm.

Keywords: Vasospasm, Stenosis, 3D printing

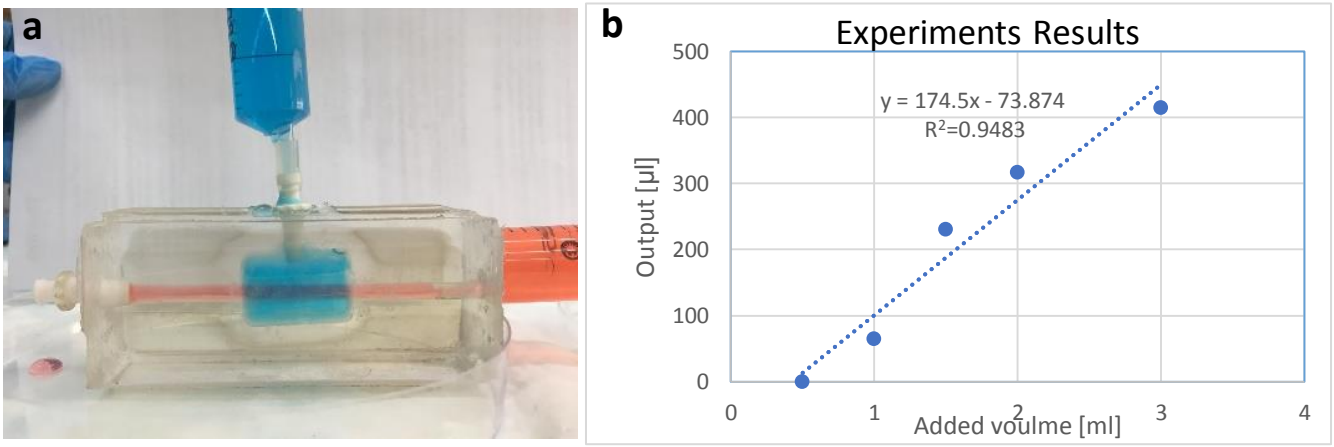

Figure 1: (a) The 3D Vasospasm System, (b) a calibration curve of the output volume as a function of the compressed added volume.

(11)

An Automatically Fully Adjustable CAD Model of a Low-cost, 3D Printed Prosthetic Hand for Trans-Radial Amputations

Valeriia Kravchik[1], Yair Herbst[2,4], Oscar Lichtenstein [1], Yoav Medan[3,4]

[1] Faculty of Biomedical Engineering, Technion - IIT, Haifa, Israel
[2] Faculty of Mechanical Engineering, Technion – IIT, Haifa, Israel
[3] Faculty of Electrical Engineering, Technion – IIT, Haifa, Israel
[4] Haifa3D organization, Haifa, Israel.

Introduction: Patients with trans-radial amputations of any age from children to adults are common in all parts of the world. Today, prosthesis is made manually for every individual patient. This method is expensive and requires a lot of time. This problem mostly harms children who quickly grow out of prosthetic hands, and as a result, constantly need a cheap and practical solution. Other patients who will benefit from designing a low-cost and adaptable prosthesis are: patients in US with no insurance to cover the cost of producing expensive models; residents of third world countries with an undeveloped economy, and even patients in Israel who straggle to pay for expensive prosthesis and have to wait for a long time for them to be produced.

Methods: 3D printing is useful since it allows for quick customization and it supports complex geometries. For the implementation of the CAD model SolidWorks was used. To assess the success of the model and its parametric representation, statistical data was collected on the anatomical proportions of humans, both healthy and with limb abnormalities. The data limit the use of the model exclusively for trans-radial amputations, when the patient has the motor function of the stump, and can perform flexion and extension movements of the elbow. Note that if the stump is too short, the prosthesis will lack the necessary support to operate.

The developed model is compatible with the requirements of 3D printing with both isotropic and anisotropic materials, like ABS and PLA.

Results: The equations were written, and the model was designed. These equations have several parameters which are measured before production and allow the engineer to 3D print the model quickly according to the specialties of the patient's anatomy. These parameters also allow to set several other requirements such as tolerance and the actuation string tension.

Keywords: Trans-Radial Prosthesis, Adjustable 3D Printed Arm Model, Low-Cost Production

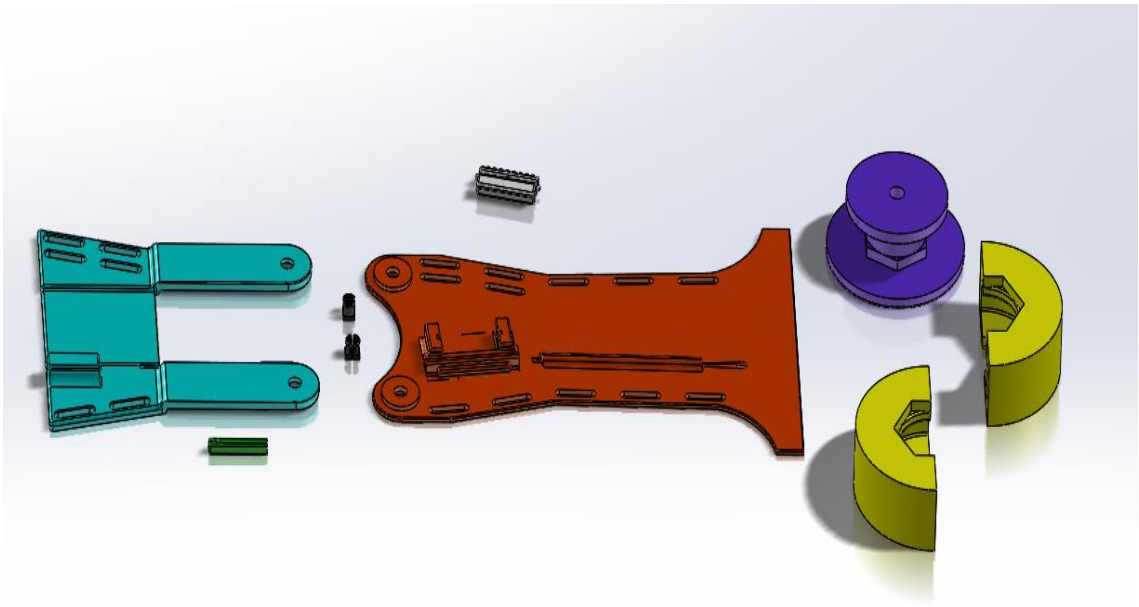

Figure 1: Printing Table - Full Arm Model

Laboratory of Bioelectric and Bioenergetic Systems

(12)

Detection of Genetic Disorder Mechanisms in the Sinoatrial Node via ECG and Advanced Signal Processing

Ofri Goldenberg[1], Yuval Ben Sason[1], Ido Weiser-Bitoun[1], Aviv Rosenberg[2], Yael Yaniv[1]

[1]Faculty of Biomedical Engineering, Technion - IIT, Haifa, Israel
[2]Faculty of Computer Science, Technion - IIT, Haifa, Israel

Introduction: The sinoatrial node (SAN) is the primary pacemaker of the heart, which determines the rhythm of heart contractions. Genetic disorders are one of the reasons for SAN-related pathologies. Although they are rare, such disorders can be life threatening. However, in some cases they can only be conclusively diagnosed by genetic testing. We aim to develop a novel algorithm to detect genetic disorders affecting the heart, in particular HCN4 and SCN5A mutations affecting the SAN, only by analyzing beat-intervals calculated from ECG recordings.

Methods: Our data includes clinical Holter ECG recordings (24 hours) of a family affected by HCN4 mutation (n=4, under age 50), a family affected by SCN5A mutation (n=5, under age 45), healthy individuals (NSR PhysioNet database) (n=7, under age 35) and a set of various other cardiac disorders which serves as an advanced negative control, taken from PhysioNet databases. Both genetic-disordered ECG recordings were kindly provided by the Inherited Arrhythmia Clinic, Cardiology Department, Rambam Healthcare Campus.
We applied heart rate variability (HRV) analysis to the ECG data by analyzing the beat-intervals between adjacent R-peaks. Analysis was carried out using a computational platform, PhysioZoo and mhrv toolbox. For each recording we extracted 27 features, including time, frequency and non-linear HRV metrics. We implemented different types of Machine Learning classification methods, both binary and multiclass.

Results: We managed to classify the four groups using a Softmax classifier with L1 regularization and second order features transformation. We report a sensitivity of 83.70%. By classifying the HCN4 group from all other groups and only from the healthy patients, we managed to have success rate of 95.22% and 98.23%, respectively. By classifying the SCN5A group from all other groups, we managed to have success rate of 84.93%.

	Classifier	Accuracy	Success
HCN4 vs. NSR	Logistic Regression	98.99%	**98.74%**
HCN4 vs. All	Logistic Regression	97.42%	**95.22%**
SCN5A vs. All	Logistic Regression	85.40%	**84.31%**
Multiclass	Softmax with L1 and second order features	87.73%	**83.70%**

Table 1: Summary of the best performance algorithms

Conclusions: By comparing the feature properties of all groups, we found that the HCN4 group has exceptional values in some features which enable us to accurately classify it. The features we found most significant for this classification are related to heart rate (RR, AVNN, RMSSD, SEM, pNN50, PIP, PAS), RR interval frequency power (HF-Norm-Lomb, LF-Norm-Lomb, Total-Power-Lomb and VLF-Power-Lomb) and non-linear analysis (SD1, SD2). Interestingly, we can indicate the connection between the pathophysiological mechanism of HCN4 disorder and these features, that point out high variability of the heart rate and bradycardia. This connection is based on the autonomic nervous system compensation for the deteriorated SAN function.

The SCN5A classification was more challenging, but still we managed to identify most of these ECG recordings mainly by using frequency domain and non-linear features.
Our research project is a proof of concept for genetic disorder diagnosis by Machine Learning analysis of ECG recordings. Future improvements can make our algorithm a clinical tool for healthcare providers and domestic use.

Keywords: Sinoatrial node, genetic disorders, ECG, Machine Learning.

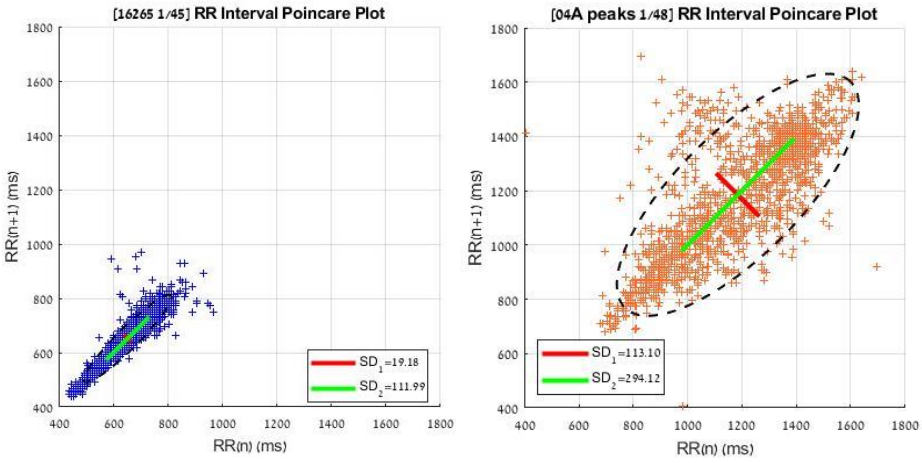

Figure 3: Poincare plot of healthy patient (a) and HCN4 patient (b)

(13)

An Accessible Recording System for Analyzing Cardiovascular Signals

Gal Shleifer[1], Yael Pistunovich[1], Aviv Rosenberg[2], Ido Weiser-Bitoun[1], Yaron Blinder[3], Yael Yaniv[1]

[1]Biomedical Engineering Faculty, Technion - IIT, Haifa, Israel
[2]Computer Science Faculty, Technion - IIT, Haifa, Israel
[3]Zebra Medical Vision Ltd, Kibbutz Shfayim, Israel

Introduction: The ability to monitor physiological parameters relating to the human body can contribute to better patient supervision. One of the leading methods for cardiac diagnosis and monitoring is electrocardiogram (ECG), which measures the electrical activity of the heart. Despite improvements in its mobility, most ECG devices are not fully accessible for continuous patients monitoring. Wearables, such as smartwatches, are becoming a common method of continuous cardiac monitoring during everyday activities. Such devices generally measure the blood pressure with a photoplethysmogram (PPG) sensor. Analysis of the pulse watch signal can be used to detect heart beats represented in the signal by mechanical changes of the blood flow. The time-variations between adjacent heartbeats, which can be measured from ECG, reflect the heart rate variability (HRV). HRV is a reliable indicator of many physiological factors modulating the normal rhythm of the heart and can be used to diagnose cardiac diseases. The ability to use PPG signals for this purpose, instead of ECG, could provide much benefit in terms of availability, but has yet to be proven. We aim to explore this use of PPG in our project.

Methods: We have built a system composed of several algorithms which enable us to record, synchronize and analyze ECG and PPG signals simultaneously. The system records a PPG signal from a pulse watch, PPG signal from a finger probe sensor, and lead I of ECG signal.
We recorded these three datasets from 10 healthy volunteers, aged 20-30. Then, we analyzed the data in order to temporally synchronize all three signals using our cross-correlation algorithm to overcome the physiological and technical differences between the measuring methods.
Afterwards, using our algorithm, we detected the intervals of each heartbeat in all three signals in order to calculate the HRV measures.

Results: We statistically analyzed the signals to evaluate the similarity between the HRV parameters derived from the pulse watch PPG and those derived from the ECG and the finger probe PPG. We observed a 1.7% mean relative error between the number of peaks in the ECG and pulse watch PPG. Additionally, we found a high similarity (mean relative error under 5%) for 5 HRV measures calculated from each measuring device.

HRV measure	relative error [%] watch PPG↔ECG
RR	1.33
AVNN	2.32
LF peak lomb	0.16
LF power lomb	1.35
VLF norm lomb	4.64

Conclusions: The system we built has successfully recorded ECG and PPG signals simultaneously, while demonstrating high peak-detection accuracy. Based on 5 HRV measures, we have shown high correspondence between pulse watch-derived PPG signals and ECG signals (as the gold standard). Thus, PPG-based monitoring devices could serve as a tool for measuring the heart rate properties and cardiac activity. These results serve as an additional step forwards to use pulse watch as a tool for continuous cardiac monitoring.

Keywords: Heart Rate Variability, ECG, PPG, Blood Volume Pressure.

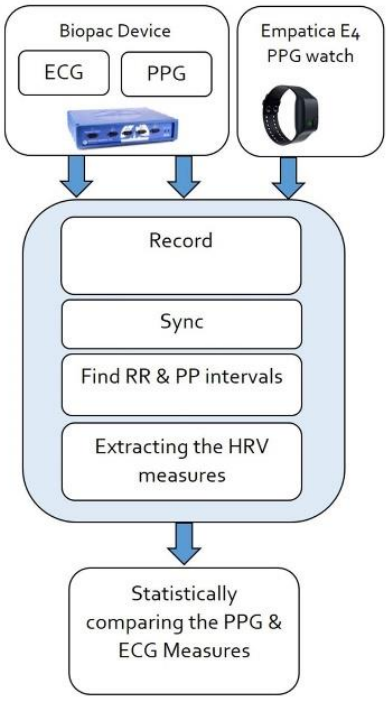

Figure 4: Project work flow.

(14)

Super Resolution Dynamic Microscopy a 3D CNN Solution

Yan Ziselman[1], Mordechai Vaknin[1,3], Elias Nahme[1,2], Yoav Shechtman[1,2]

[1] Faculty of Biomedical Engineering, Technion - IIT, Haifa, Israel
[2] NanoBioOptics lab, Biomedical-Engineering, Technion - IIT, Haifa, Israel
[3]Faculty of Medicine, Technion - IIT, Haifa, Israel

Introduction: In conventional microscopy, the spatial resolution of an image is bounded by Abbe's diffraction limit, corresponding to approximately half the optical wavelength. Super resolution methods, specifically localization microscopy, namely photo-activated localization microscopy and stochastic optical reconstruction microscopy have revolutionized biological imaging in the last decade, enabling the observation of cellular structures at the nanoscale. Although Deepstorm is successful with static samples, it fails for dynamic samples. This is the problem we tackled in our project by first creating simulated videos of microtubules and then using them to train a network of our own, to produce super resolution videos of microtubule movement.

Methods: The lack of real data had us write our own simulator to produce video files that resemble PALM based data acquisition of microtubule movement. Using the framework laid out by PyTorch, we implemented a convolutional neural network architecture that is suited to the task at hand. After reaching subpar results we Revisited the architecture design – convolutional GRU. To train our models we used resources provided freely by google. In each experiment, the model was trained using a training set of 7000 samples and validation set of 3000 samples. To try and handle generalization problems we encountered, we also experimented with training our models using new data in each iteration.

Results: Our model managed to increase the resolution of videos with an error of 5% according to L1 distance and 20% according to MS-SSIM distance. We believe that given better computational power we would have been able to experiment further and produce a model able of reaching our goals and perhaps even move forward to the next intended step of simulated videos emulating the process of dynamic instability in microtubules. Unfortunately, the lack of literature in applying CNNs efficiently to video data and length of computational tasks (which lasted more than a week per experiment) made it very hard for us to reach our goals in time.

Conclusions: Though our results might still be preliminary and rely on simulated data of global movement, our research shows that the subject selected (microtubule movement) should hold up in the greater scheme of our plan. Dynamic instability moves at rates slower than the time resolution constraints of PALM and our network will, hopefully, be capable of predicting this motion. We believe that our model will achieve its goal, to produce videos of microtubule dynamic instability in a resolution greater than physical limitations, it just won't be at the end of this year.

Keywords: Microtubules, Neural Network, Super resolution.

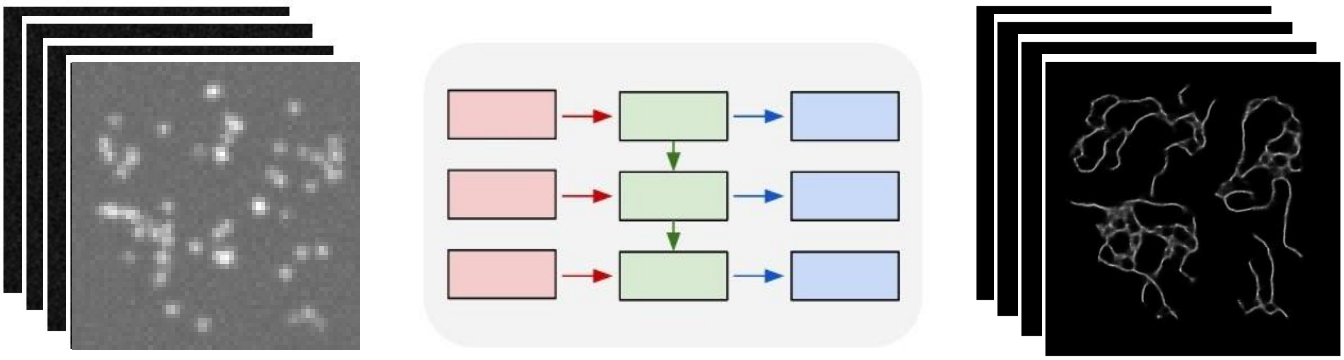

Figure 1: feeding the network with simulated PALM videos of microtubules, results in a video file reconstruction of resolution better than conventional microscopy.

(15)

Recognition in Ultra-Sound Images of the Region of Interest Around the Left Ventricle with Convolutional Neural Networks (CNN)

Ilan Misano[1], Michal Tamir[1], Alon Begin[1], Yaron Blinder[2], Dan Adam[1]

[1]Biomedical Engineering Faculty, Technion - IIT, Haifa, Israel
[2]Zebra Medical Vision Ltd. - Shefayim, Israel

Introduction: Echocardiography is the imaging of the heart function by ultrasound. It has become more and more used (+3% year over year) in the diagnosis, management, and follow-up of heart diseases. Lately, many researches are being done for the development of algorithms to automatically segment cardiac ultrasound images and analysing ventricles' movements and size. However, these algorithms can't optimally segment the heart from an entire ultrasound image, because the images include also other organs, structures and are often noisy, so the tools can miss the region of interest. Moreover the ultrasonography include various limits on its field of view, causing the images to be inconsistent in orientation and consequently making the segmentation task more challenging.The project's objective is to use convolutional neural networks to detect the position and angle of left ventricle from long-axis 2-chamber ultrasound images.
Once this primary detection is achieved, the existing segmentation algorithms can act in an ideal situation (on the cropped and straightened region of interest), approaching in this way a complete pathway to automatic heart function diagnostics from ultrasound images.

Methods: the project is based on the neural network provided by Lei Liu et al., 'DRBox', which is based on the 'caffe' framework (Matcaffe and Pycaffe). DRBox uses truncated VGG-net with modification on the layers to reach angle detection. Matlab was used for ground truth labelling, results displaying and evaluation. The dataset was composed by 210 pictures, each from a different patient, all from a GE ultrasound machine in Rambam Hospital. Images were taken during the end systolic phase. Results were evaluated via the Intersection Over Union analysis.

Results: The proposed architecture did not perform precisely on a newly trained network due to limitations in the computational power and iterations number. When applied specific conditions to the network on the desired number of outputs, it reached a top precision of 32% in the intersection over union calculation (figure 1). The CNN performed inferiorly when using the pre-trained model provided by the DRBox paper reaching a maximum precision of 22%. The DRBox tool outperformed the SSD and caffe frameworks on airplane, ship and vehicles detection (see table below):

Method	Dataset	BEP(%)	AP(%)	mAP(%)
Faster R-CNN	Ship	79.20	82.29	85.63
	Vehicle	71.60	75.55	
	Airplane	98.07	99.06	
SSD	Ship	82.72	82.89	89.68
	Vehicle	83.13	87.59	
	Airplane	97.74	98.56	
DRBox	Ship	94.62	94.06	94.13
	Vehicle	86.14	89.07	
	Airplane	98.62	99.28	

However, it failed perform precisely on ultrasound images because of their noisy nature, low computational power used and small dataset.

Conclusion: The current CNN (DRBox) detection is not precise enough for further segmentation; however, results can be dramatically improved by enhancing the computation power (and consequently the training iterations number), dataset size and processing time. Moreover, by using transfer learning, networks previously trained on other tasks can provide a good starting point for an additional training on ultrasound images, leading to a more precise bounding box placement. This framework represents a promising tool that, by working on the mentioned parameters and methods, could bring us nearer to a complete pathway to automatic segmentation and heart disease diagnostics from ultrasound images.

Keywords: Cardiac Ultra-Sound, Left Ventricle Labelling, Tilted Bounding Box, Rotation Invariant Detection, Convolutional Neural Network

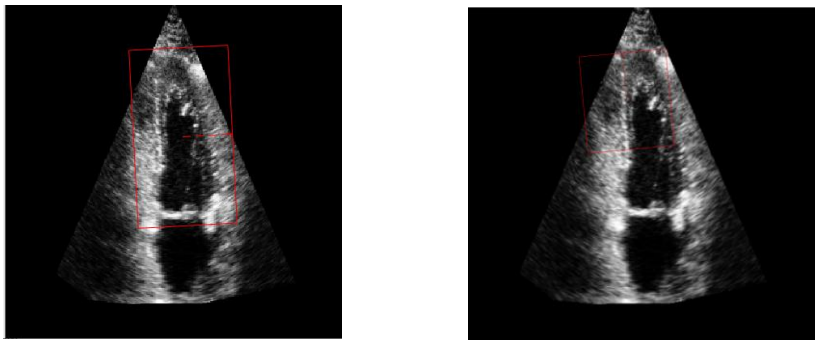

Figure 1: Manually positioned box around left ventricle (red box, left) vs. automatic labelling by the trained CNN (red box, right).

(16)

Semi-Automatic Classification of Short-Axis Views of the Left Ventricle in Ultrasound Recordings

Mor Finestine[1], Salomé Attali[1], Alon Begin[1], Ido Farhi[1], Yaron Blinder[2], Dan Adam[1]

[1] Biomedical Engineering Faculty, Technion - IIT, Haifa, Israel
[2] Zebra Medical Vision Ltd

Introduction: Nowadays, over 30 million echocardiograms are performed every year worldwide, each of them creating 40 to 70 ultrasound videos as an output. In order to make a diagnosis, the physician must review the recordings and perform additional. The evaluation of the performance of the left ventricle of the heart, and thus the detection of heart diseases, must first rely on an automatic classification of the different cross-sections of the heart. Previous work has already been done to classify the long-axis cross-sections of the left ventricle. However, no algorithm has yet been built for the classification of the three short-axis cross-sections: the mitral valve view, the papillary muscles view, and the apical view.

Methods: An image processing algorithm was built and performed on healthy patients' recordings (n=47) in order to classify the three short-axis cross-sections of the left ventricle. At first, the mitral valve view was detected using a semi-automatic evaluation of the pixel values in a specific region of interest. A level-set algorithm was then applied on the remaining views using an edge-based active contour model, allowing the extraction of major features of the left ventricle: its area and the ratio between its radius and the shortest distance from its center. The latter indicates the presence of papillary muscles along the wall of the ventricle. Finally, a decision tree was implemented based on these features in order to distinguish between the apical and the papillary muscles views.

Results: The highest performance was achieved for the mitral view with a sensitivity of 98% and a specificity of 98%. The apical view scored a sensitivity of 89% and a specificity of 93% and the papillary muscles view scored a sensitivity of 85% and a specificity of 93%.

Conclusion: The classification of the different short-axis cross-sections of the left-ventricle of the heart was successfully achieved by a semi-automatic image processing-based algorithm. For further improvement, machine learning methods could be implemented allowing the fully automatic extraction of additional features of the left ventricle of the heart, which would increase the ability to efficiently diagnose millions of patients suffering from heart diseases.

Keywords: ultrasound, classification, short-axis, left-ventricle

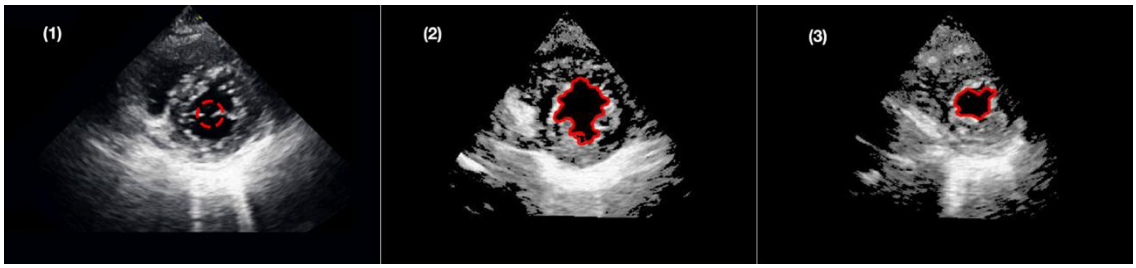

Figure 1: The three cross-sections of the left ventricle. (1) Mitral valve view: high pixel values in the region of interest. (2) (3): Papillary muscles and apical views: level-set output showing the detection of the left ventricle

(17)

Respiration Signal Detection in Thermal Images Using Deep Learning and Image Processing

Noam Freundlich[1], Gadi Mendel[1], Tomer Czyzewski[2], Amit Livneh[1] and Yonatan Savir[2]

[1] Faculty of Biomedical Engineering, Technion - IIT, Haifa, Israel
[2] Department of Physiology, Biophysics & Systems Biology, Technion- IIT, Haifa, Israel

Introduction: In 2017, around 3600 cases of Sudden Unexpected Infant Death (SUID) were listed in the U.S. The objective of this project is to be able to use affordable thermal camera in order to detect the breathing signal of a sleeping infant. While breathing, the temperature of the infant's nostrils changes as can be seen in the thermal camera .If the baby stops breathing for some reason, our system's goal is to detect this drastic abruption and alert the parents, thus increasing the survival rate of the infant.

Methods (see figure 1):
1) We used "Flir One Pro" thermal camera in order to obtain our thermal data.
2) Using Transfer Learning method to train an existing CNN (*convolution neural network*), VGG16, on 2 classes: "face" and "no face". The entire database consists of 1500 images, 900 of the "no face" class and 600 of the "face" class. The training process used 70% of the database, and the validation process used 30%.
3) Taking the output of the previous stage, and delimiting the face in a "face" class image using the RCNN (*Regional CNN)* method.
4) Taking the output of the previous stage (a cropped image of only the face area), and using Cascade Object Detector to delimiting the nose area.
5) Recording a person breathing for a certain time duration using the thermal camera (video).
6) Inserting the frames of the recorded video in the designed system and obtaining the breathing signal by averaging the value of the pixels in the delimited area (nose) which correlates to the breathing process.

Results: We will address the results of each stage in the Methods section separately:
2) Face Recognition: This stage showed the best results. We were able to correctly classify 100% of the validation data. Additionally, testing the performance of the CNN on a dataset of over 200 new images also achieved 100% success rate.
3) Face Detection: This stage also showed prominent results, successfully delimiting the face in over 90% of the validation data.

4) Nose Detection: Detecting the nose in a thermal image of the face using the Cascade Object Detection method. We were able to successfully identify the nose area in a thermal image of a face. In a video of over 200 frames we were able to detect a nose successfully in 100% of the frames, and detect the nostrils in 95% of them.

6) Breathing signal acquisition: We were able to obtain the breathing signal from the cropped nose region of the thermal image (as seen in fig. 1 plot), and by comparing the signal to the video itself we were able to determine that the acquisition of the breathing signal is accurate and matches the reality.

Conclusions: Overall, we have shown the feasibility of obtaining a breathing signal from a thermal video using low end IR camera.

Keywords: Facial Recognition, Thermal Imaging, Breathing Detection

Figure 1: A flow chart that describes step by step how the designed system works.

(18)

Advanced Methods in Functional Mapping of the Cerebral Cortex During Awake Craniotomy

Shaked Ron[1,2], Amit Livneh[1], *Firas Mawase[1] and *Omer Zarchi[3]

[1] Faculty of Biomedical Engineering, Technion - IIT, Haifa, Israel
[2] Faculty of Medicine, Technion - IIT, Haifa, Israel
[3] Intraoperative Neurophysiological Service, Rabin Medical Center, Israel
*equally contributed

Introduction: Awake craniotomy is a complicated procedure mostly conducted in cases of surgeries related to brain tumors or severe epilepsy. During this procedure, the patient's cerebral cortex is being mapped according to functionalities in order to minimize the probability of post-surgery complications. Today, the gold standard method for cortical mapping is electrocortical stimulation (ECS). In ECS, cerebral regions are stimulated while the patient is observed to identify any changes in the mental or physical performance. An emerging method for intraoperative cortical mapping utilizes electrocorticography (ECoG) and high-gamma frequencies for the purpose of brain mapping. Such "passive" (no stimulation induced) mean of mapping carries hope for safer procedure and may become an effective mean for depicturing brain networks involving the functioning of interest intraoperatively. Yet, many questions regarding this technique need to be clarified. Here we discuss the development of a closed loop decision support system (DSS) to synchronize tasks fulfilled by the patient with ECoG signal recorded intraoperatively (fig. 1).

Methods: The Neuro Omega™ (by Alpha Omega) is an intraoperative neuromonitoring device capable of simultaneously record and stimulate the nervous system, combining ECS and ECoG, with the capacity of an external MATLAB (by MathWorks) based control. A made-from-scratch pseudo-brain phantom used to pre-develop and verify system's capabilities. MATLAB was used to develop a user-friendly graphic user interface (GUI). Different analysis methods were used to distinguish task-related activity from resting-state signal: Power Spectrum Density, Spectral Energy Integral and statistical T-test, while analysis was done in both time and frequency domains.

Results: The developed DSS is capable of presenting tasks to the patient while recording synchronized neural activity, processing the data and producing a projection of the result – an intraoperative functional map. We managed to develop a closed loop system that is a step towards more efficient and safer craniotomies.

Conclusions: Creating an intraoperative functional map using ECoG seems to be possible and efficient. Yet, as mentioned beforehand, this field is to be further explored before it will replace the current gold standard (ECS) completely. In order to further improve the efficiency of functional mapping using ECoG, experience and data should be collected using the discussed DSS in future surgeries. We have made the first step towards accomplishment of our goal to produce a more efficient and safer intraoperative functional mapping of the cerebral cortex.

Keywords: Awake Craniotomy, Electrocorticography, Intraoperative Functional Mapping, Electrocortical Stimulation.

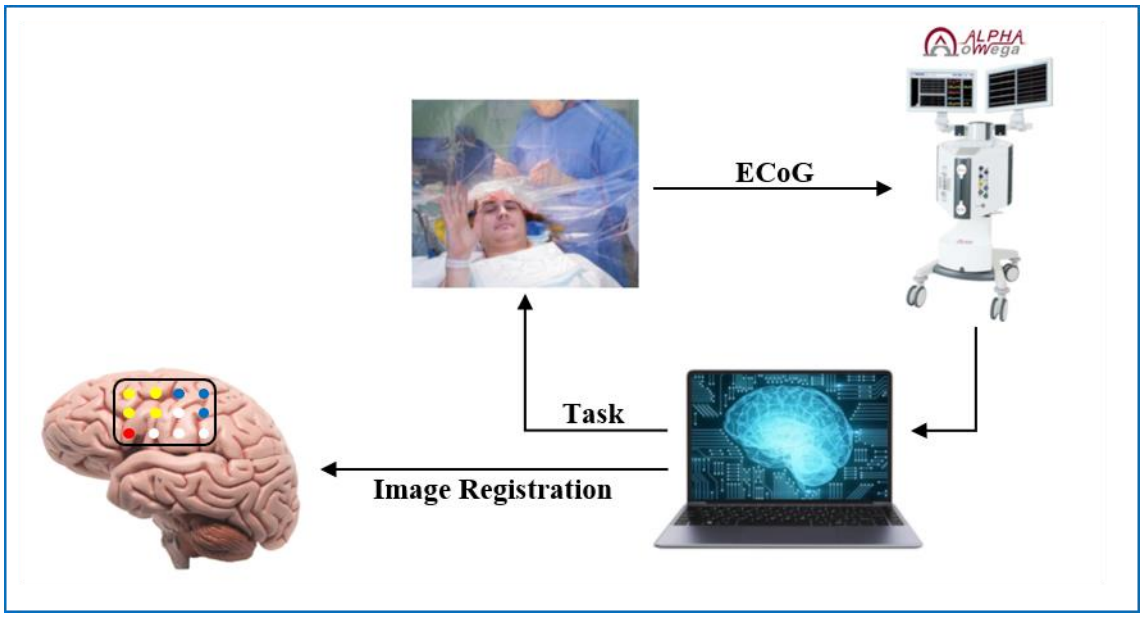

Figure 1 (System Design): the main computer displays tasks to the awake patient intraoperatively and simultaneously acquires data from the Neuro Omega system to produce the functional map of the brain.

(19)

Examining Cardiopulmonary Interactions Prior to a Cardiac Arrest in Children

Yonatan Prat[1,3], Yuval Barzilai[1,3], Amit Livneh[1], Danny Eytan[2,3]

[1]Faculty of Biomedical Engineering, Technion - IIT, Haifa, Israel
[2]Pedriatic Intensive Care Unit, Rambam Health Care Campus
[3]Faculty of Medicine, Technion - IIT, Haifa, Israel

Introduction: The cardiac and pulmonary physiological sub-systems affect each other via multiple bi-directional mechanic and reflex loops. Multiple studies have linked these modulations to the cardiovascular (volemic for example) status of the patient, expected response to treatment and sympathetic tone. We hypothesized that an impending critical event, such as a cardiac or a pulmonary arrest, in one of these systems might arise from a significant dysfunction of the feedback relations (the risk of cardiac arrest increases dramatically during post-operation recovery). We sought to examine the modulations caused by the respiratory cycle on the blood pressure and heart rhythm in populations of patients that underwent cardiac arrest while monitored in the pediatric intensive care unit (PICU).

Methods: 26 patients from the PICU were monitored, each one for at least 3 hours prior to and after cardiac arrest. Using vital sign data – invasive arterial blood pressure, ECG and respiratory impedance we measured the respiratory induced modulations in systolic blood pressure and heartbeat synchronization. From these signals we extracted the instantaneous respiratory phase (using the Hilbert transform), beat by beat absolute systolic blood pressure and relative change in blood pressure and the exact timing of the systolic beat. The respiratory induced modulations in systolic blood pressure were characterized by the phase amplitude coupling method (PAC): Each patient's data were divided to 18 segments, and in each, we chose the most artefact free subsegment of three minutes (See figure 1). We also examined the distribution of systolic beat times relative to the respiratory phase to examine the extent of synchronization.

Results: We generated the phase amplitude coupling graphs for each patient in the period surrounding cardiac arrest. From these graphs we extracted several descriptive statistics. The first is the relative mean systolic blood pressure during a respiration cycle (using a polynomial fit). The second one is the root mean square error (RMSE) between the relative systolic blood pressure curve and the pressure distribution around that curve that estimates the extent of variability in those modulations. The third statistic is the distance between the probability distributions of the systolic beat times over a region of one respiratory cycle (using Kulback Liebler and Earthmover Distance statistic tools).

Conclusions: Prediction of cardiac arrest in PICU patients has a crucial effect on the child's prognosis. The model we have described above provides a new insight on the cardio-pulmonary feedback systems and may serve in the future to construct better algorithms to arrest prediction and to elucidate the mechanism leading to such a catastrophic event.

Keywords: Cardio-pulmonary feedback; Cardiac arrest; Pediatric intensive care; Phase amplitude coupling;

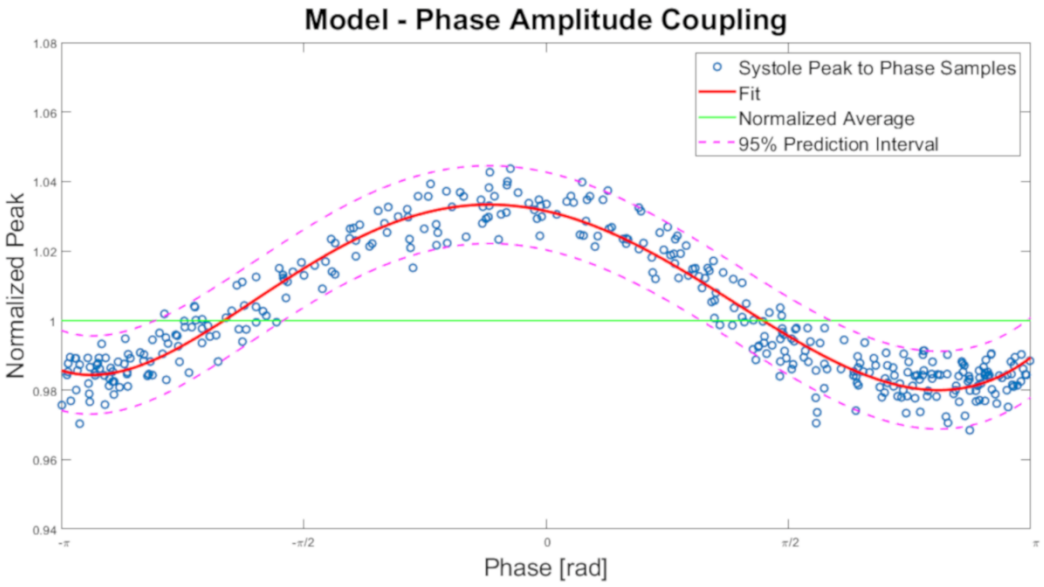

Figure 1: Each systole peak sample was matched with the phase of the respiration at any specific time. The absolute pressure at each peak was standardized to the mean of all peaks during the 180 seconds.

(20)

Estimation of Thermal Acoustic Response of Brain Tissue to Focused Ultrasound Implementing Coded Excitation

Alisa Komleva, Yevgeniya Shteynman, Daniel Dahis, Amit Livneh, Haim Azhari

Faculty of Biomedical Engineering, Technion - IIT, Haifa, Israel

Introduction: Brain treatments using Focused Ultrasound offer a range of noninvasive transcranial therapies. The acoustic energy distribution during the treatment may induce temperature elevation in the tissue, therefore, thermal monitoring is essential. Magnetic Resonance Imaging is currently the adopted monitoring modality, but its high operational costs and strong magnetic field limit its accessibility. Ultrasound, on the other hand, constitutes a non-ionizing, cost-effective, portable and highly available imaging modality. However, ultrasound is commonly not used for transcranial applications, due to the difficulty of the detection of the signal reflected from within the skull. Here we hypothesize that by implementing Coded Excitation, which are a set of pre-prepared phase or amplitude modulated signals, it is possible to develop a transcranial acoustic thermal monitoring tool for Focused Ultrasound treatments.

Methods: Four fresh bovine brains were dissected into white and cortical matter. Specifically, three samples of white matter and seven cortical matter samples were prepared. Each sample was gradually heated to 48℃, and then immersed in degassed water of room temperature. Thermocouples were inserted inside the samples for temperature monitoring. While the tissue cooled down, specially coded pulses were transmitted to the samples. The transmissions were done by a coaxially embedded transducer within a focused ultrasound transducer. Four different set of experiments were implemented. The first two used a water-based phantom with/without a flat bovine bone mimicking the skull and the others using brain tissues with/without bone as well. The scans yielded a temporal series of A-lines which were later used for post processing. The sample's speed of sound was extracted using a *Golay* coded excitation decompression algorithm and plotted as a function of temperature.

Results: A characteristic trajectory was between speed of sound and temperature was observed for each of the scanned materials. The relation obtained for the water-phantom was compared to the theoretical relation with Mean Error of 4.1 m/sec. After the insertion of the bone, this Mean Error increased to 9.51 m/sec. Experiments with brain showed that the speed of sound for cortical matter increased as temperature was elevated while an inverse relation was observed for white matter.

Conclusions: A monotonic increase of the speed of sound as a function of temperature in water for the measured temperature range was obtained using coded excitations with a relatively low error. Much noisier results were obtained for the cortical matter, with noise ratio.

Keywords: Focused Ultrasound, Coded Excitation, Speed of Sound, Thermometry

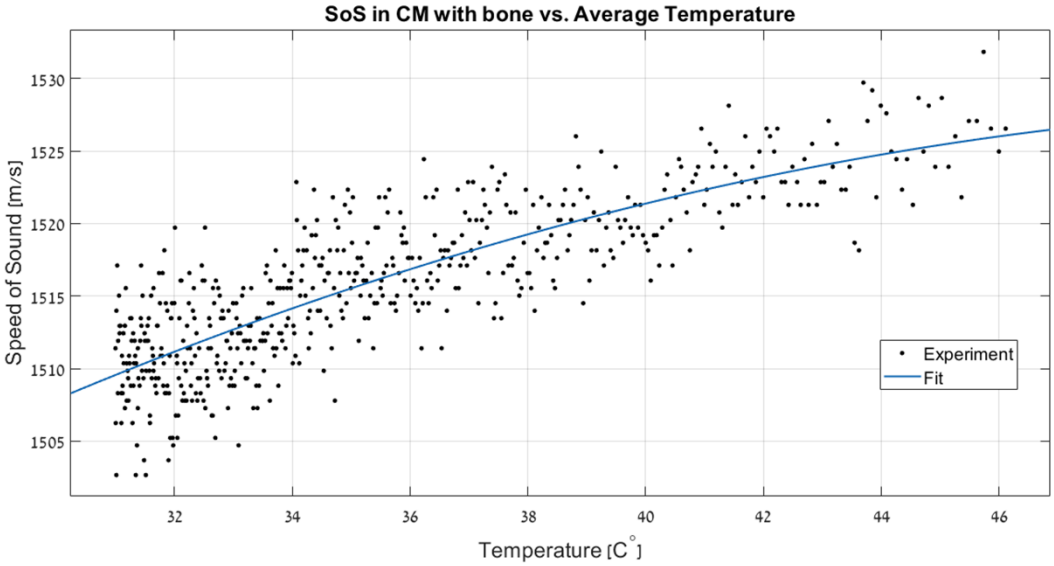

Figure 1: Speed of Sound vs. Temperature for one sample of bovine Cortical Matter, with addition of the bone.

(21)

Automatic Identification of the Optimal Reconstruction Phase for Coronary Arteries CT Images

Maya Israel[1], Noam Moshe[1], Amit Livneh[1], Eran Langzam[2]

[1]Faculty of Biomedical Engineering, Technion - IIT, Haifa, Israel
[2]Philips Healthcare Ltd., Israel

Introduction: Cardiac CT is a common heart-imaging procedure that is being used to visualize the heart anatomy. It can be useful in the diagnosis of suspected functional or anatomical heart problems, such as coronary heart disease. The images are generally reconstructed in multiple cardiac phases because different coronary arteries may be better visualized in some phases than in others, due to the periodic cardiac motion. The accurate diagnosis is strongly depended on the quality of the coronary arterial tree images, hence, it is very time consuming for the radiologist to manually select the optimal reconstruction phase of the scan. The purpose of our project was to create an algorithm that can automatically identify of the optimal reconstruction phase for coronary arteries CT images. This will help obtaining faster and improved reconstruction phase selection process and enables the radiologist to receive the best quality images immediately.

Methods: An automated algorithm was developed to select the optimal reconstruction phase for each of the main coronary arteries: Left Anterior Descending Artery (LAD), Left Circumflex Artery (LCX) and Right Coronary Artery (RCA). Patients' datasets were reconstructed in different steps of the R-R interval. All reconstructed phases were segmented using Philips Comprehensive Cardiac Analysis (CCA application) and the spatial coordinates of the center lines of each vessel at each phase were extracted. For each vessel at each reconstructed phase, two parameters were calculated, and a "phase score" was derived accordingly. The parameters are related to the length of the vessel and to the motion of the vessel. The "Phase score" is based on a weighted combination of the two parameters. This flow was repeated twice: first pass of reconstruction phases with 10% steps, provided a rough estimation of the quiet phase. Second pass of reconstruction phases with 1% steps, resolved to the range and fine-tuned derived value. Proof of Concept was applied on datasets of three patients overall; calculation of one patient was done on the 10% steps only. Specialist reviewer discriminated the optimal reconstruction phase for each patient, per each vessel. This was compared with the algorithm selection, to determine the algorithm's performance.

Results: The best phase that was selected by the specialist for the first reconstructions stage was 80% for all patients and all the vessels (9 samples overall). When applying

the 10% steps only, the best phase that was selected by the algorithm output was aligned with the specialist selection at 7 out of the 9 vessels (combining the different patients). The average error for this stage was evaluated as 5.56%. For the second part of the algorithm, the best phase that was selected by the specialist was 80% for all the vessels of the first patient and 78% for all the vessels of the second patient (6 samples overall). When applying the 10% steps, followed by the 1% tuning, the algorithm output was aligned with the specialist selection at 2 out of the 6 vessels. The average error for this stage was evaluated as 1.83%.

Conclusions: A proof of concept of an algorithm that can automatically identify of the optimal reconstruction phase for coronary arteries CT images was implemented. The algorithm can help obtaining faster and improved reconstruction phase selection process and enables the radiologist to receive the best quality images immediately. The algorithm demonstrated promising results, yet the small number of cases that were processed holds back from getting a clear assessment of its accuracy.

Keywords: Cardiac CT; Coronary Arteries; Motion Artifacts; Reconstruction Phase;

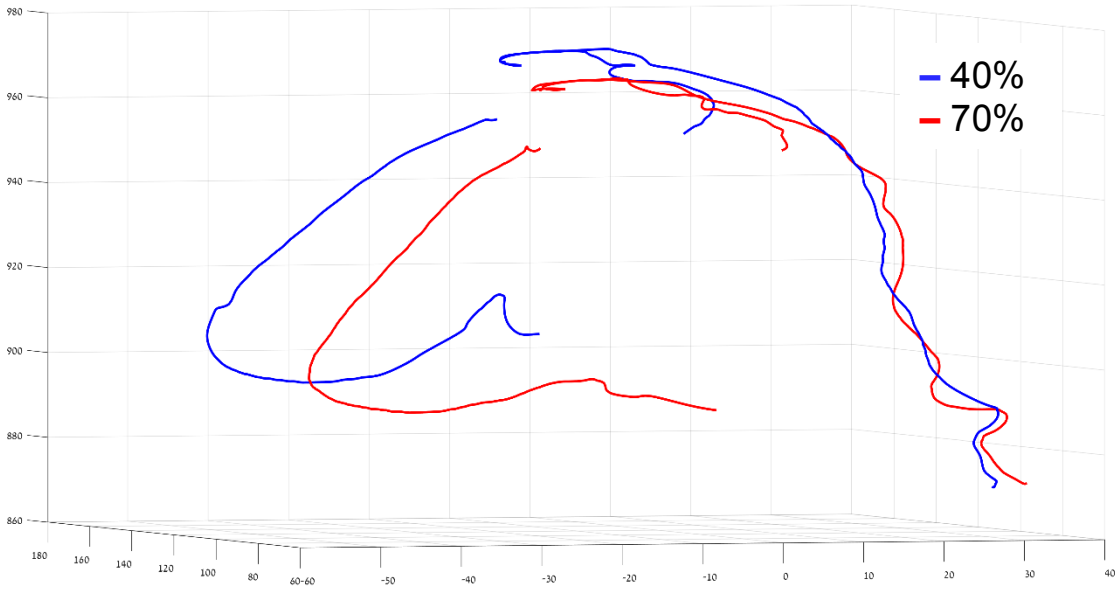

Figure 1: Comparison of reconstruction of the coronary arteries tree in 2 phases. This represents the differences between the phases, e.g. in the length or location, as expected.

שלום רב,

אנו שמחים להציג בפניכם את תקצירי הפרויקטים של הסטודנטים המסיימים לימודיהם בשנה זו, שנת תשע"ט.
הפרויקט, המבוצע ע"י סטודנטים בשנת הלימודים האחרונה, מהווה את גולת הכותרת של לימודיהם לתואר בהנדסה ביו-רפואית.
במסגרת הפרויקטים מביאים הסטודנטים לידי ביטוי את הידע והכלים שרכשו במהלך השנים בתחומי ההנדסה, המדע והרפואה.
מטרת הפרויקטים הינה לתת מענה לצרכי הפיתוח והמחקר של חברות העוסקות בתחום ההנדסה הביו-רפואית, תוך עמידה בסטנדרטים המקובלים ובמקביל, לתת ניסיון ואתגר מקצועי לסטודנטים המסיימים ולעודד השתלבותם בתעשייה הביו-רפואית.
לפרויקטים חלק חשוב בעידוד היזמות בקרב הסטודנטים, וחלקם אף מובילים להקמת חברות הזנק ורישום פטנטים.

פרויקטים אלו מהווים נדבך מרכזי בחזון הפקולטה, לחתור לבניית גשר למצוינות ובמה לקשרים ושיתופי פעולה ארוכי טווח בין האקדמיה והחברות המובילות בתעשייה.

הפקולטה מאחלת הצלחה לסטודנטים המסיימים, ומקווה לראותם בעתיד נוטלים חלק פעיל בפרויקטים חשובים אלו כמנחים מהתעשייה.

בברכה,
פרופ' שולמית לבנברג , דיקנית הפקולטה
פרופ'מ נתנאל קורין, אחראי קורס פרויקטים

הפקולטה להנדסה ביו-רפואית
טכניון

כנס
פרויקטים

26 ביוני, 2019

תקצירים